

2010-01-01

Generation Of High Resolution Radar Signals Using Three Dimensional Chaotic Flows

Chandra Sekhar Pappu

University of Texas at El Paso, cspappu@miners.utep.edu

Follow this and additional works at: https://digitalcommons.utep.edu/open_etd



Part of the [Electrical and Electronics Commons](#)

Recommended Citation

Pappu, Chandra Sekhar, "Generation Of High Resolution Radar Signals Using Three Dimensional Chaotic Flows" (2010). *Open Access Theses & Dissertations*. 2560.

https://digitalcommons.utep.edu/open_etd/2560

This is brought to you for free and open access by DigitalCommons@UTEP. It has been accepted for inclusion in Open Access Theses & Dissertations by an authorized administrator of DigitalCommons@UTEP. For more information, please contact lweber@utep.edu.

GENERATION OF HIGH RESOLUTION RADAR SIGNALS USING THREE DIMENSIONAL CHAOTIC FLOWS

CHANDRA SEKHAR PAPPU

Department of Electrical and Computer Engineering

APPROVED:

Benjamin C. Flores, Ph.D., Chair

Ricardo Von Borries, Ph.D.

Berenice Verdin, Ph. D.

Helmut Knaust, Ph.D.

Patricia D. Witherspoon, Ph.D.
Dean of the Graduate School

Copyright ©

by

Chandra Sekhar Pappu

2010

Dedication

To my father Mr. S. R. Murthy Pappu, my mother Mrs. Kameswari Pappu, my brother Aditya Pappu, my best friend-sister Anusha Badveeti and my Professor Dr. Benjamin C. Flores for their Continuous encouragement and efforts in completing this work

GENERATION OF HIGH RESOLUTION RADAR SIGNALS USING CHAOTIC FLOW

by

CHANDRA SEKHAR PAPPU, B. Tech

THESIS

Presented to the Faculty of the Graduate School of

The University of Texas at El Paso

in Partial Fulfillment

of the Requirements

for the Degree of

MASTER OF SCIENCE

Department of Electrical and Computer Engineering

THE UNIVERSITY OF TEXAS AT EL PASO

August 2010

Acknowledgements

It was all because of god's grace. As a child I dreamed of starting and ending my career as a professional technician serving for my country. I knew that I should pursue higher education in order to fulfill that dream. After 15 years I had a very special opportunity to pursue quality education in area of defense. My heart felt thanks to Dr. Benjamin C. Flores in trusting me and giving an opportunity to do research under him. Holding several academic and administrative positions, anyone who spent time with Dr. Flores would tell that he is also uncharacteristically modest and completely down to earth. His encouragement, motivation, advice and support were essential to the completion of this thesis. Dr. Flores being a father figure to me, apart from my educator he supported me mentally and financially throughout this work. It would not be easy for me if Dr. Flores was not there behind this research. Thank you for believing me and giving me a golden chance to work with you making me live my dreams.

My special thanks to Dr. Ricardo Von Borries for helping me in improving my work. I express my sincere appreciation to Dr. Von Borries, who helped me in enhancing my knowledge in probability and random signals which is back bone for this research.

I am so grateful to Dr. Helmut Knaust for taking special interest and helping me in research whenever it is necessary. Also thank you for advising me to improve this quality of work.

Dr. Berenice Verdin is one of the best people I ever met. She taught me how to be like a researcher, scientist and encouraging me whenever I had a tough task in front of me. Thank you for your continuous help and mentoring me during this work.

Special thanks to my parents who always encouraged me and dedicated their lives in pursuing my higher studies. Its always fun being with my brother Aditya whose presence make me feel happy. One of the most important people in my life is my best friend and sister Anusha, who always supported me whenever I was stressed and tensed. She was special friend to me when I was an Undergrad, speaking about everything left in this world. She is the person who identified my enthusiasm and spirit

in me for doing research in this field of interest. Thank you for your friendship, undoubtedly you will be my greatest friend and sister I ever had.

Finally I appreciate my very good friends Nikhil Roger, Keerthi Cheekoty and Harish Bayyavarapu for their help and encouragement in other various things. Thanks for Christopher Rodriguez and Connie Gamboa for being very nice to me and flexible about my schedule during my work at the School of Nursing which was compatible with the time needed for this research. Last but not least, thanks for all who are behind this successful completion of work.

Abstract

The purpose of this project is to investigate the system parameter and certain signal processing techniques to achieve wide bandwidth and frequency agility in order to build a high resolution radar. The technique relies on the output of an n -dimensional ($n > 2$) non-linear system that exhibits chaotic behavior.

Firstly, the compressed Lorenz attractor is considered which has a set of three state variables x , y and z and three control parameters ρ , β , and σ . By varying ρ and β as function of time highly chaotic parameter space region is simulated such that chaotic signal behaves optimally.

For comparison purpose we introduced the Lang-Kobayashi attractor which also has a set of three state variables the electric field e , its phase component ϕ and the excess carrier number z and two main control parameters L and η for. The FM signals are generated from both the attractors using anyone of the state variables as an instantaneous frequency.

In both cases, we demonstrated that the obtained FM signal is ergodic and stationary and that the time samples exhibit an invariant probability density function. The corresponding pseudo-phase space trajectories reveal themselves as a strange attractor that may take on the shape of a Mobius strip depending on the time evolution of the signal.

A time-frequency analysis of the FM signal shows that the spectrum is centered on a time-dependent carrier frequency. Thus, the FM signal has a high time-bandwidth product and fractional bandwidth similar to that of a chirp. However, the carrier frequency continuously shifts in a linear or quadratic pattern that folds over range of $(-f_s/2, f_s/2)$.

The time averaged autocorrelation has main width inversely proportional to bandwidth of the FM signal. The ambiguity surface reveals that the optimized chaotic based FM signal has shape as a set of mountain ridges with low sidelobes both in range and Doppler which is desirable for obtaining high resolution radar and range-Doppler imaging.

Table of Contents

Acknowledgements.....	v
Abstract.....	vii
Table of Contents.....	viii
List of Tables	x
List of Figures.....	xi
Chapter 1: Introduction.....	1
1.1 Problem Statement.....	1
1.2 Previous work	1
1.1 Proposed Solution, Goal and Methodology.....	2
Chapter 2: Strange Attractors, Lyapunov Exponent and Highly Chaotic Parameter Space Region.....	3
2.1 Introduction.....	3
2.2 Chaotic Signals	3
2.3 Lyapunov Exponent.....	4
2.4 Lorenz Attractor and Highly Chaotic Parameter Space Region.....	5
2.5 Lang-Kobayashi Attractor	12
Chapter 3: Behavior of Chaos-Based Frequency Modulated Signals	17
3.1 Frequency Modulated Signals	17
3.2 Chaos Based Frequency Modulated Signals	17
3.3 Block Diagram of Chaos Based FM Signal Generation.....	20
3.4 Ergodicity, Time-Frequency Analysis and Spectra.....	21
3.5 Bandwidth Improvement Based on Time-Frequency Distribution	30
Chapter 4: Statistical Analysis of Chaos-Based Frequency Modulated Signals	35
4.1 Time Bandwidth Product of the Chaos Based Frequency Modulated Signals.....	35
4.2 Fractional Bandwidth of the Chaos Based Frequency Modulated Signals	37
4.3 Ensemble mean Autocorrelation of the Chaos Based Frequency Modulated Signals.....	42
4.4 Ensemble mean Ambiguity Surface of the Chaos Based Frequency Modulated Signals.....	44
Chapter 5: Conclusions.....	49

References.....	52
Vita.....	54

List of Tables

Table 2.1: Parameter specification of the Lorenz attractor at different regions	6
Table 2.2: Parameter specification of the Lang-Kobayashi attractor.....	13
Table 4.1: Comparison of results obtained for different types of chaos based FM signal.....	44

List of Figures

Figure 2.1: Lorenz attractor for reference parameter values of $\beta= 2.67$, $\rho=28.00$ and $\sigma = 10.00$.	8
Figure 2.2: Pseudo phase space trajectory of $x(n)$ for reference parameter values	8
Figure 2.3: Time behavior of $x(n)$ for reference parameter values	9
Figure 2.4: Probability density function of $x(n)$ for reference parameter values	9
Figure 2.5: Highly chaotic parameter space region of the Lorenz attractor as function of β and ρ	10
Figure 2.6: Lorenz attractor for optimized parameter values of $\beta= 9.00$, $\rho=172.00$ and $\sigma= 10.00$	10
Figure 2.7: Pseudo phase space trajectory of $x(n)$ for optimized parameter values	11
Figure 2.8: Time behavior of $x(n)$ for optimized parameter values	11
Figure 2.9: Probability density function of $x(n)$ for optimized parameter values	12
Figure 2.10: Lang-Kobayashi attractor for $L= 0.30$ and $\eta=0.09$	14
Figure 2.11: Second projection of the Lang-Kobayashi attractor	15
Figure 2.12: Pseudo phase space trajectory of the Lang-Kobayashi attractor	15
Figure 2.13: Time behavior of $e(n)$ of the Lang-Kobayashi attractor	16
Figure 2.14: Probability density function of $e(n)$ of the Lang-Kobayashi attractor	16
Figure 3.1: Block diagram of the Chaos based FM signal generation	21
Figure 3.2: Ergodic behavior of the Lorenz chaotic FM signal for reference parameter values	22
Figure 3.3: Ergodic behavior of the Lorenz chaotic FM signal for optimized parameter values	23
Figure 3.4: Ergodic behavior of the Lang-Kobayashi chaotic FM signal	23
Figure 3.5: Behavior of pseudo phase space trajectory and spectrum of the Lorenz chaotic FM signal depending on time-frequency distribution	25
Figure 3.6: Behavior of pseudo phase space trajectory and spectrum of the Lang-Kobayashi chaotic FM signal depending on time-frequency distribution	26
Figure 3.7: Time-frequency distribution analysis of the Lorenz chaotic FM signals in different parameter space regions	27
Figure 3.8: Time-frequency distribution of the Lorenz chaotic FM signal for optimized Parameter values	28
Figure 3.9: Close up view of time-frequency distribution of the Lorenz chaotic FM signal for optimized parameter value	29
Figure 3.10: Time-frequency distribution of the Lang-Kobayashi chaotic FM signal	29
Figure 3.11: Close up view of time-frequency distribution of the Lang-Kobayashi chaotic FM signal	30
Figure 3.12: Behavior of pseudo phase space trajectory and spectrum of the Lorenz FM signal depending on slope and length of time-frequency distribution of FM signal	32
Figure 3.13: Behavior of pseudo phase space trajectory and spectrum of the Lang-Kobayashi FM signal depending on slope and length of time-frequency distribution of FM signal	33
Figure 3.14: Spectral behavior of the Lorenz chaotic FM signal for optimized parameter	34
Figure 3.15: Spectral behavior of the Lang-Kobayashi chaotic FM signal	34
Figure 4.1: Time-bandwidth product of the Lorenz chaotic FM signal for reference parameter values	36
Figure 4.2: Time-bandwidth product of the Lorenz chaotic FM signal for optimized parameter values	36
Figure 4.3: Time-bandwidth Product of the Lang-Kobayashi chaotic FM signal	37

Figure 4.4: Range of fractional bandwidth of the Lorenz chaotic FM signal for reference parameter values	38
Figure 4.5: Range of fractional bandwidth of the Lorenz chaotic FM signal for optimized parameter values	39
Figure 4.6: Range of fractional bandwidth of the Lang-Kobayashi chaotic FM signal	39
Figure 4.7: Distribution of center frequency of the Lorenz chaotic FM signal for reference parameter values	40
Figure 4.8: Distribution of center frequency of the Lorenz chaotic FM signal for optimized parameter values	41
Figure 4.9: Distribution of center Frequency of the Lang-Kobayashi chaotic FM signal	41
Figure 4.10: Ensemble mean autocorrelation of the Lorenz chaotic FM signal for reference parameter values.	42
Figure 4.11: Ensemble mean autocorrelation of the Lorenz chaotic FM signal for optimized parameter values	43
Figure 4.12: Ensemble mean autocorrelation of the Lang-Kobayashi chaotic FM signal	43
Figure 4.13: Ensemble mean ambiguity surface of the Lorenz chaotic FM signal for reference parameter values	47
Figure 4.13: Ensemble mean ambiguity surface of the Lang-Kobayashi chaotic FM signal for reference parameter values	47
Figure 4.15: Ensemble mean ambiguity surface of the Lang-Kobayashi chaotic FM signal	48

Chapter 1: Introduction

The term chaos is used to describe nonlinear, deterministic and bounded phenomena that possess unpredictable behavior or disorder. In an instance of time, phenomena may vary considerably for an infinitesimal change in initial conditions, causing an exponential divergence in the final outcome [1]. In context of telecommunications and radar signal processing aspects chaos have excellent applications in spread spectrum schemes [2] and signal transmission purposes.

1.1 Problem Statement

Radar performance tends to be less than ideal for surveillance and military roles when high resolution is required under electronic counter countermeasures (ECCM) [3]. For radar imagery applications, the transmitted signal should look like wide band noise [4] with a spectrum that is uniformly spread over a wide bandwidth. Also, the signal should be constructed such that it yields high resolution in the range-Doppler plane [5], has little likelihood of intercept and intrusion, and is easy to generate. In some cases the pulse width of transmitted signal should be increased simultaneously maintaining adequate range resolution. This can be resolved by using pulse compression techniques which depends on the time-bandwidth product of transmitted signal.

In order to overcome all the above mentioned limitations, we propose using a chaos based Frequency Modulated (FM) signal where the instantaneous frequency varies randomly over some prescribed bandwidth. The typical task of having a large bandwidth, high time-bandwidth product and frequency agility can be achieved by using this chaos based FM signal [6].

1.2 Previous Work

Extensive research has been done since mid-20th century on the use of the random FM signals for radar applications [7]. Applications of a random FM signals for radar imaging have been given in [8-9]. In previous work done by Flores [10-12], it was considered the use of chaotic maps to construct a chaotic FM signal with applications in radar imaging. Most of the research was concerned with target imaging. Also a sufficient condition for the chaotic FM signal was provided for the case of a one dimensional map [13]. The analysis was based on the Lyapunov exponent that explains the presence of

chaos in the signal. It was proven that the chaos based FM signals have features similar to that of random FM signals but is not exactly random in nature [12].

1.3 Proposed Solution, Goal and Methodology

In this research effort, we are interested in optimizing the bandwidth of a chaotic signal. We propose the usage of output of n -dimensional ($n > 2$) non-linear system that exhibit chaotic behavior for the construction of FM signals. In particular, we consider the Lorenz attractor and vary the control parameters in order to obtain highly chaotic signal that behaves optimally [15]. Later we use a compression factor for the Lorenz attractor such that it oscillates with high frequency similar to that of the Lang-Kobayashi attractor used by Verdin [16-17], where the signal possess high bandwidth and range resolution.

Since the obtained chaotic signals are noise like in nature, we expect the FM signals that are constructed using the chaotic variables also have similar desirable properties. We use any one of the state variables from both the attractors as an instantaneous frequency to generate a wideband realization FM signal. We compare the Lorenz chaotic FM signal with the Lang-Kobayashi chaotic FM signal and we verify that both of these signals have significant features in terms of time frequency analysis, time bandwidth product, fractional bandwidth, power spectral spread, mainlobe width of autocorrelation, ambiguity function, range resolution and Doppler resolution.

This thesis is organized into five chapters. Chapter two shows the chaotic properties of the attractors used to generate the chaos based FM signal. Chapter three discusses behavior of the FM signal constructed in highly chaotic parameter space region compared to that of other parameter space regions. Chapter four shows the obtained time-bandwidth products, fractional bandwidths, ensemble autocorrelation and ambiguity functions of both the chaos based FM signals. Chapter five summarizes the conclusions of this work.

Chapter 2: Strange Attractors, Lyapunov Exponent and Highly Chaotic Parameter Space Region

2.1 Introduction

The orbit or a trajectory of a chaotic system will be drawn into a limited region of state space as time goes to infinite, where upon it moves to a deterministic but unpredictable manner on a fractal object called strange attractor. A signal is said to be chaotic if its time behavior exhibit fractal nature. Similarly its three dimensional flow should appear as a strange attractor rather than a stable origin, transient chaos or a point attractor. Another interesting feature of an attractor is its pseudo-phase space trajectory should resemble its own attractor. This feature is known Diffeomorphism which is essential condition for a system to be chaotic. The Lorenz attractor and the Lang-Kobayashi attractor are examples of strange attractors possessing all above mentioned chaotic properties.

2.2 Chaotic Signals

A signal is said to be chaotic if its time series plot exhibit aperiodic and apparently random behavior. Chaotic systems are mathematically modeled by non-linear differential equations. Three descriptors are needed to characterize a chaotic system: the time evolution equations, the values of the parameters describing the systems, and the initial conditions. Chaotic systems are highly sensitive to initial conditions; a very small variation in initial condition produces an exponential difference in output. In addition, a small change in the control parameters can cause chaos to disappear or to reappear. For simplicity, consider a three-dimensional chaotic flow with variables $x(t)$, $y(t)$ and $z(t)$. Let $x[(n+1)\Delta t]$, $y[(n+1)\Delta t]$ and $z[(n+1)\Delta t]$ be the discrete versions of the variables from which three FM signals are generated. In each case, the instantaneous frequency will be proportional to

$$x[(n+1)\Delta t] = g[x(n)\Delta t] \quad (2.1)$$

$$y[(n+1)\Delta t] = g[y(n)\Delta t] \quad (2.2)$$

$$z[(n+1)\Delta t] = g[z(n)\Delta t] \quad (2.3)$$

where the sampling index is $n = 0, 1, 2, \dots$.

Here Δ represents the sampling interval and $g(.)$ represents the folding function that gives relation between the present and previous values of trajectories. This folding function is chosen in a way that the samples $\{x_0, x_1, x_2 \dots x_n\}$, $\{y_0, y_1, y_2 \dots y_n\}$ and $\{z_0, z_1, z_2 \dots z_n\}$ of (2.1), (2.2) and (2.3) exhibit fractal behavior.

2.3 Lyapunov Exponent

The chaotic behavior of a system is quantified in terms of the Lyapunov exponent, which measures the degree of divergence of the state-space orbit of system when it forms a strange attractor. Strange attractor is an appearance of chaos in nonlinear dynamical system. A system with three state variables will have three Lyapunov exponents $\lambda_1 \geq \lambda_2 \geq \lambda_3$ [1]. Chaotic nature of a system can be determined if λ_1 is positive irrespective of magnitude. The degree of divergence is going to be high if λ_1 has high value. In the particular case of 3-dimensional maps, the Lyapunov exponent can be calculated by using the following algorithm:

1. Start with an initial condition X_{a_0}, Y_{a_0} and Z_{a_0} . The initial condition has to be inside of the attractor. This is called the unperturbed orbit a.
2. Choose a second initial condition separated from the initial conditions of orbit 'a' by d_0 in any direction X_{b_0}, Y_{b_0} and Z_{b_0} . This is called the perturbed orbit b.
3. Iterate the delay differential equations one time step for each set of initial conditions.
4. Determine the new separation between orbits d_1 . The separation is calculated by using

$$d_1 = \sqrt{[(X_a - X_b)^2 + (Y_a - Y_b)^2 + (Z_a - Z_b)^2]}$$

5. Evaluate $\lambda_1 = \frac{1}{n} \sum \log\left(\frac{d_1}{d_0}\right)$ which is the local Lyapunov exponent.
6. Readjust the initial conditions of orbit b hence the separation between the orbits is d_0 .
7. Repeat step 3 to 6 to obtain an average of the Lyapunov exponent.

In the case that the dynamical equations of the system are not know the Lyapunov exponent can be calculated by using the “poor man’s Lyapunov exponent”. The poor man’s Lyapunov exponent is equal to the inverse of the width of the main lobe of the autocorrelation function.

2.4 Lorenz Attractor and Highly Chaotic Parameter space Region

Initially in this project we propose use of the Lorenz attractor that has three state variables; x , y and z which are governed by three control parameters the Rayleigh number ρ , Temperature constant β , and the Prandtl number σ [18]. The mathematical expression for the Lorenz system is given as

$$\frac{dx(t)}{dt} = \sigma[y(t) - x(t)] \quad (2.4)$$

$$\frac{dy(t)}{dt} = x(t)[\rho - z(t)] - y(t) \quad (2.5)$$

$$\frac{dz(t)}{dt} = x(t)y(t) - \beta z(t) \quad (2.6)$$

Due to parameter complexity of the Lorenz system we limited the sampling frequency to 1 MHz initially. In order to oscillate the Lorenz attractor fast, to make signal smooth enough and to increase bandwidth of FM signal constructed using this Lorenz signal we added a new parameter called compression factor α . By adding the compression factor, the sampling frequency is increased to 50 GHz, but the attractor becomes smoother. The new mathematical expression for the Lorenz attractor is as shown in equations (2.7), (2.8) and (2.9). In what follows, we use the compressed Lorenz attractor to compare it with an uncompressed Lang-Kobayashi attractor.

$$\frac{dx(t)}{dt} = \alpha\{\sigma[y(t) - x(t)]\} \quad (2.7)$$

$$\frac{dy(t)}{dt} = \alpha(x(t)[\rho - z(t)] - y(t)) \quad (2.8)$$

$$\frac{dz(t)}{dt} = \alpha[x(t)y(t) - \beta z(t)] \quad (2.9)$$

The most common control parameter values of the Lorenz attractor are $\beta= 8/3$, $\rho =28$ and $\sigma= 10$ [1] and the corresponding Lyapunov exponent is 0.98. Figure 2.1 shows the strange attractor of the Lorenz system for values of $\beta= 8/3$, $\rho =28$ and $\sigma= 10$. The corresponding chaotic signal is considered as reference signal and FM signal constructed based on this chaotic signal is said to be the reference Lorenz chaotic FM signal. Figure 2.2 shows the pseudo-phase Space trajectory of the Lorenz attractor for same parameter values. Figure 2.2 illustrates that the Lorenz attractor exhibits Diffeomorphism property which is an essential condition for a system to be chaotic. Figure 2.3 shows the time behavior of the Lorenz attractor exhibiting fractal nature. 2.4 shows the probability distribution of $x(n)$ at normal parameter space region. From an observation made the chaotic behavior of signal for these parameter values seems to be normal. Hence the main objective is to maximize chaotic behavior of signal from the Lorenz attractor. For that purpose the attractor is simulated at different parameter space region and measured the Lyapunov exponent and simultaneously observed their time behavior. A small change in control parameters can cause a significant change in chaos.

Table 2.1: Parameter specification of the Lorenz attractor at different regions.

Parameter values	ρ	β	σ	λ_1
Barbaroza values	22.50	0.63	3.03	0.65
Sprott values	28.00	2.67	10.00	1.01
Highly chaotic region	90.00 to 250.00	5.00 to 10.00	10.00	8.00 to 26.50

By varying the value of ρ and β as function of time, we simulated highly chaotic parameter space region by estimating the Lyapunov exponents, observing attractor and time behavior. Interestingly in this region the signal starts behaving more chaotic in nature Figure 2.5 shows the Lorenz attractor parameter space region as function of ρ and β . Highly chaotic parameter space region occurs from the values ρ equal to 150.00 to 250.00 and β from 6.00 to 10.00. The Lyapunov exponent in this region varies from 8.00 to 26.50. An infinite number of local regions can be simulated with in a small global parameter space region. Hence irrespective of the value of the Lyapunov exponent, the Lorenz attractor behaves highly chaotic in this range of parameter space region. To show that the Lorenz attractor behaves optimally in highly chaotic parameter space region we have selected control parameters $\beta = 9.00$, $\rho = 172.00$ and $\sigma = 10.00$ randomly from the highly chaotic parameter space region. Figure 2.6 shows the strange attractor of the Lorenz system for values of $\beta = 9.00$, $\rho = 172.00$ and $\sigma = 10.00$. The corresponding chaotic signal is said to be optimized signal and FM signal constructed based on this chaotic signal is said to be the optimized Lorenz chaotic FM signal. Figure 2.7 shows the pseudo-phase space trajectory of the Lorenz attractor for same parameter values of $\beta = 9.00$, $\rho = 172.00$ and $\sigma = 10.00$. Figure 2.7 illustrates that Lorenz attractor exhibits Diffeomorphism property with more orbits hence showing more chaotic nature in this parameter space region. Figure 2.8 shows the time behavior of the Lorenz attractor in highly chaotic parameter space region having more fractal nature. Figure 2.9 shows the probability distribution of $x(n)$ at highly chaotic parameter space region. By comparing the attractor and time behavior at normal parameter space region and highly chaotic parameter space region, the Lorenz attractor behaves optimally in highly chaotic parameter space region. Just above the highly chaotic parameter space region Lyapunov exponent drops drastically and corresponding attractor behaves like transient chaotic attractor.

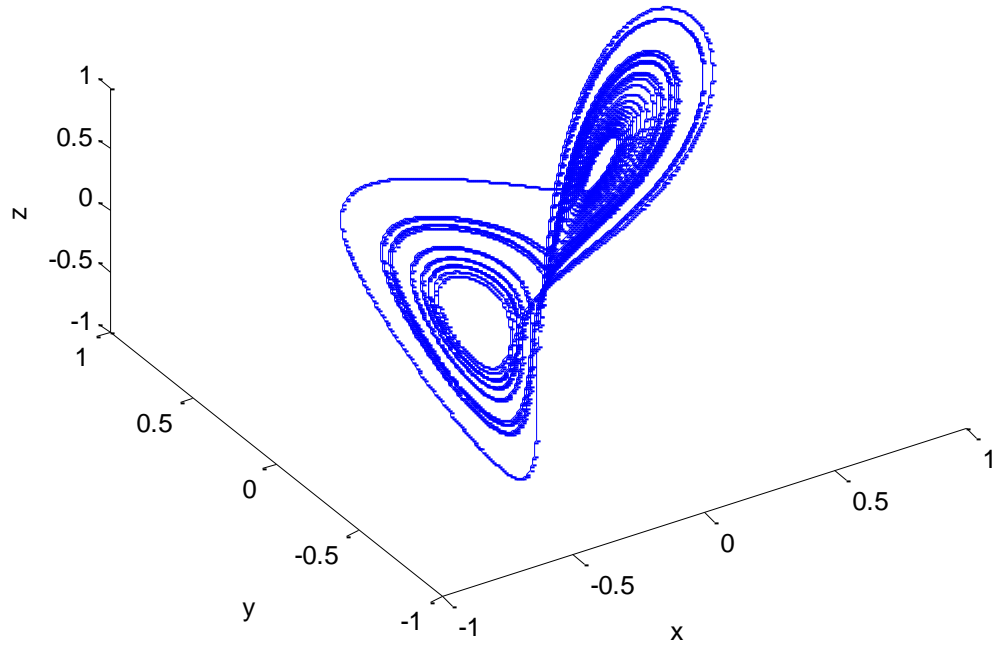


Figure 2.1: Lorenz attractor for reference parameter values of $\beta=2.67$, $\rho=28.00$ and $\sigma=10.00$.

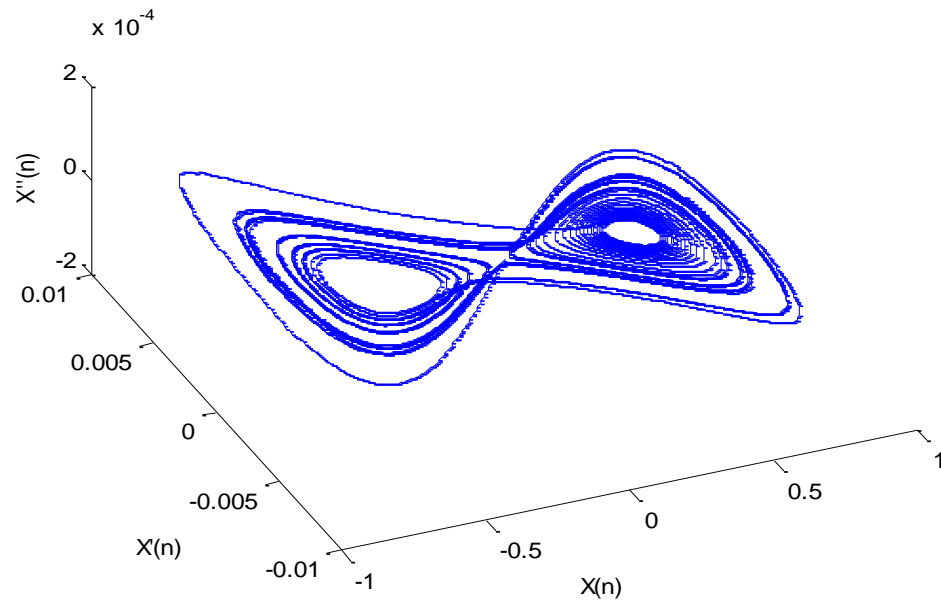


Figure 2.2: Pseudo phase space trajectory of $x(n)$ for reference parameter values.

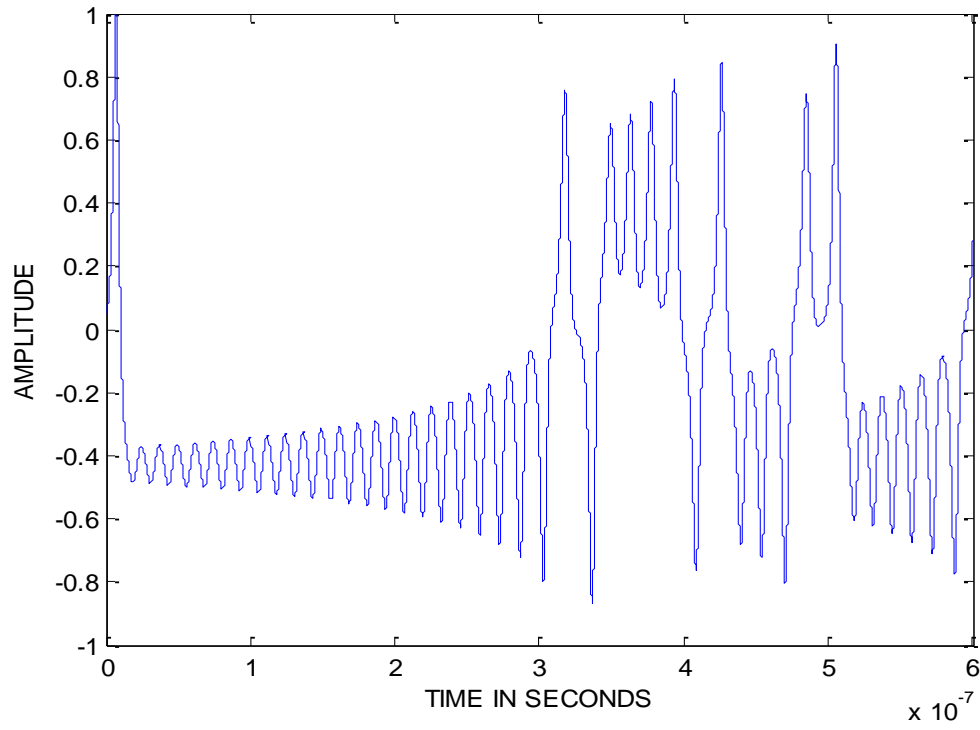


Figure 2.3: Time behavior of $x(n)$ for reference parameter values.

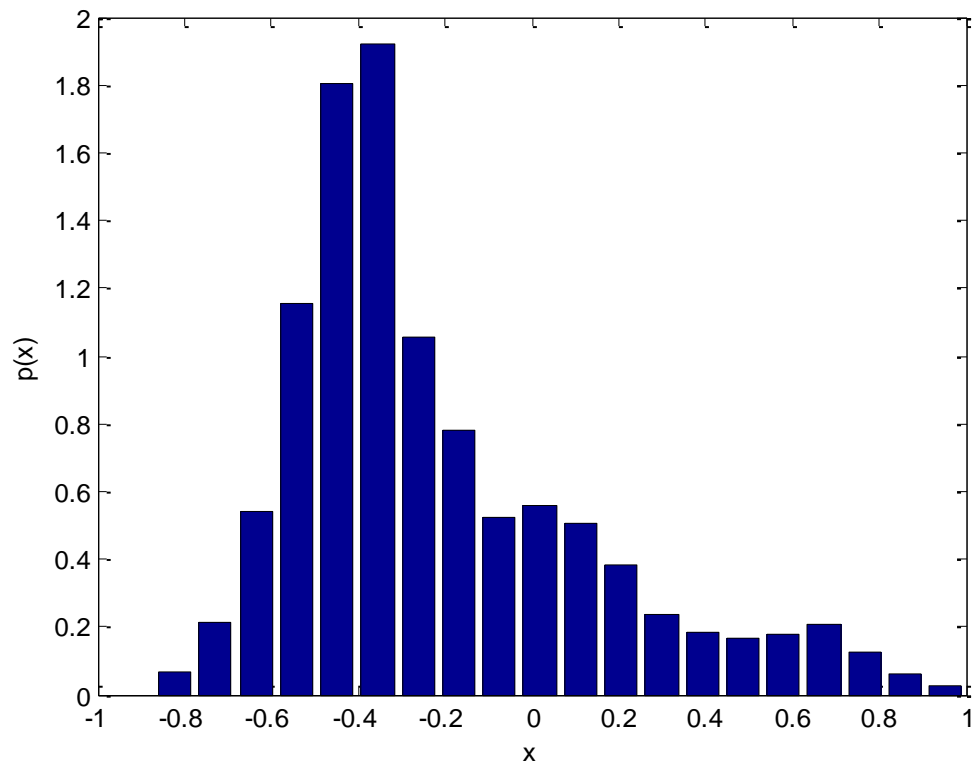


Figure 2.4: Probability density function of $x(n)$ for reference parameter values.

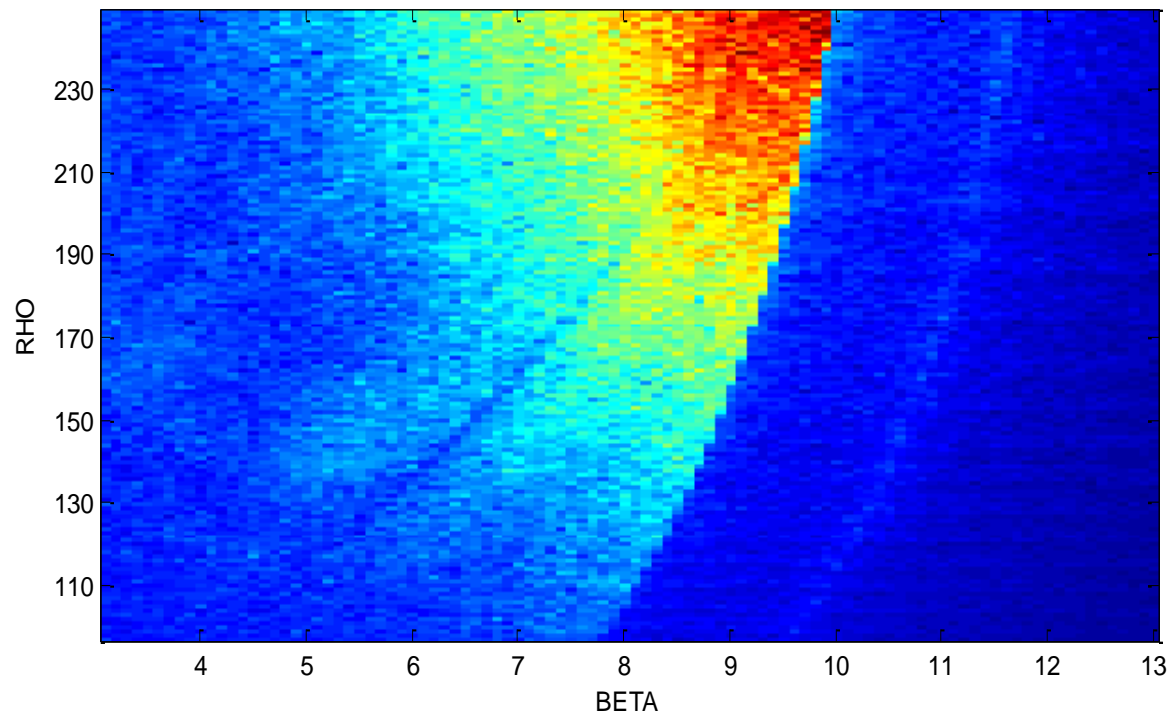


Figure 2.5: Highly chaotic parameter space region of the Lorenz attractor as function of β and ρ .

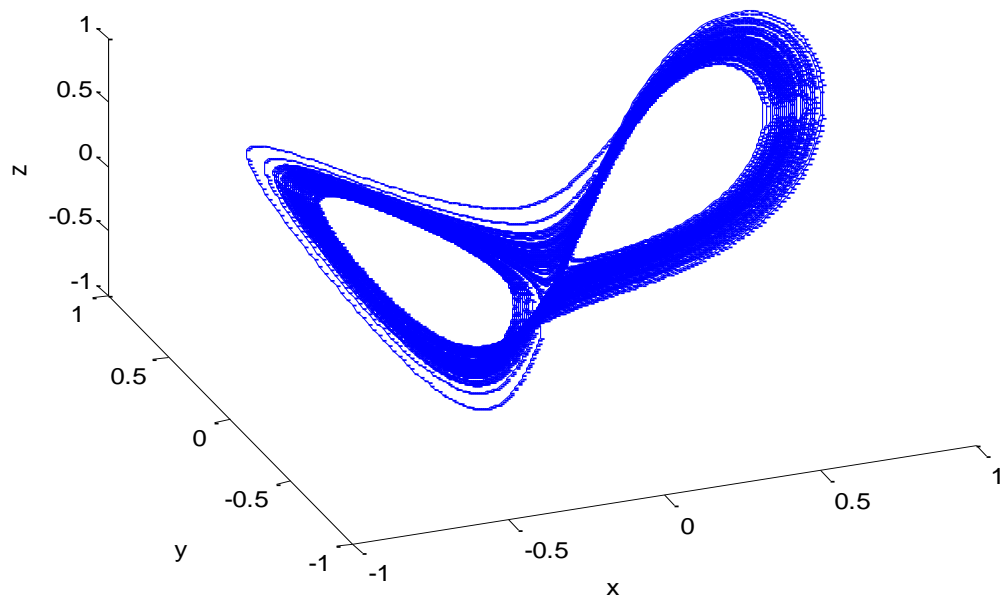


Figure 2.6: Lorenz attractor for optimized parameter values of $\beta=9.00$, $\rho=172.00$ and $\sigma=10.00$.

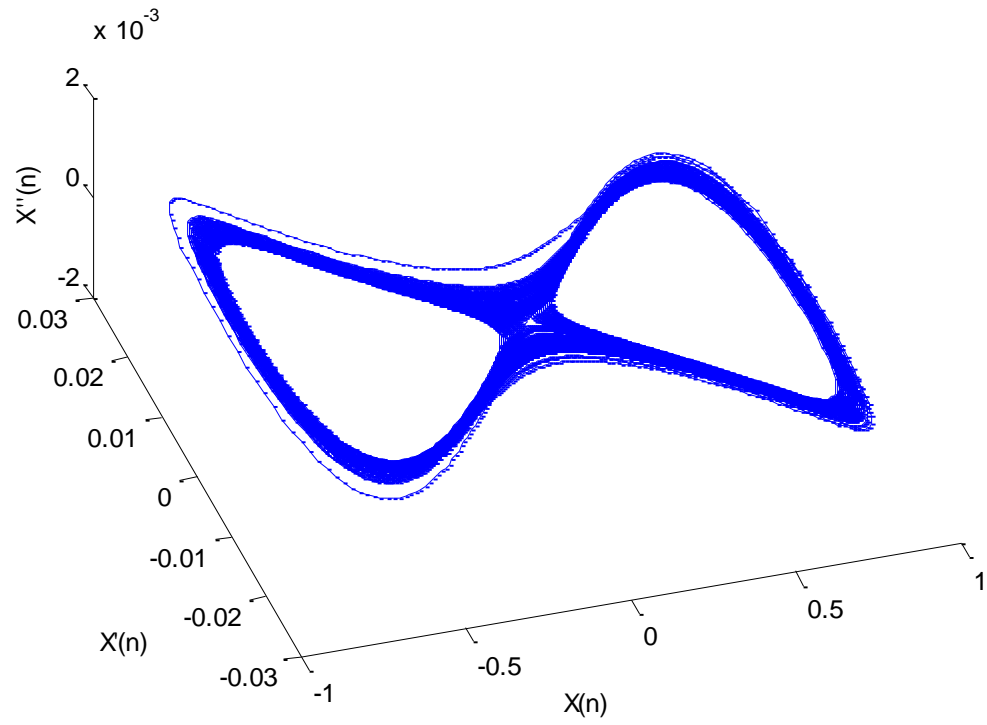


Figure 2.7: Pseudo phase space trajectory of $x(n)$ for optimized parameter values.

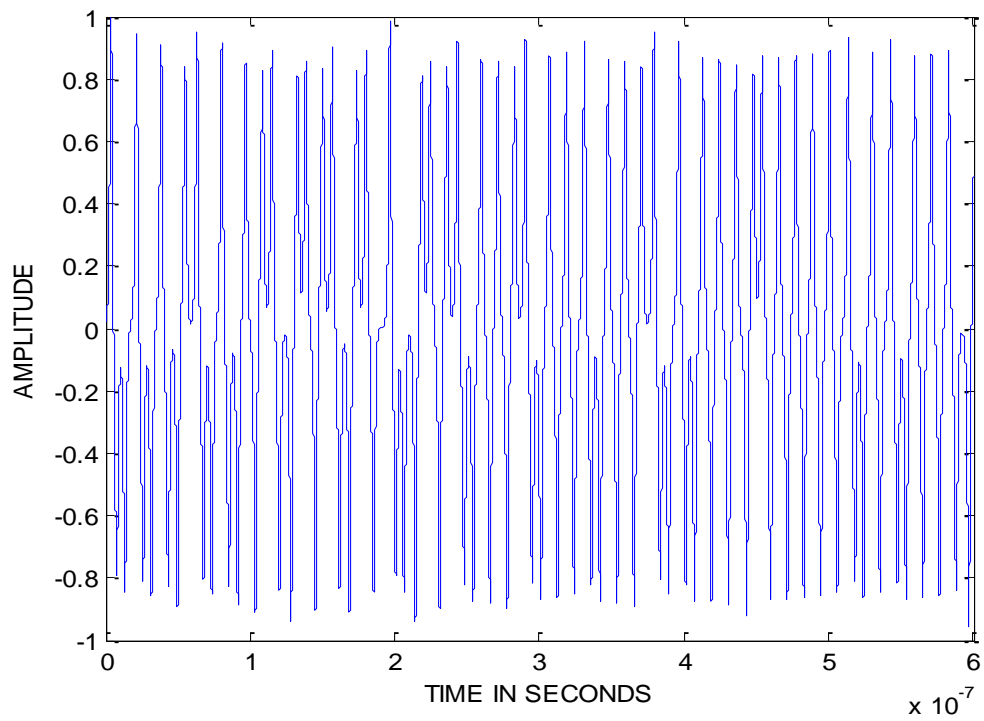


Figure 2.8: Time behavior of $x(n)$ for optimized parameter values.

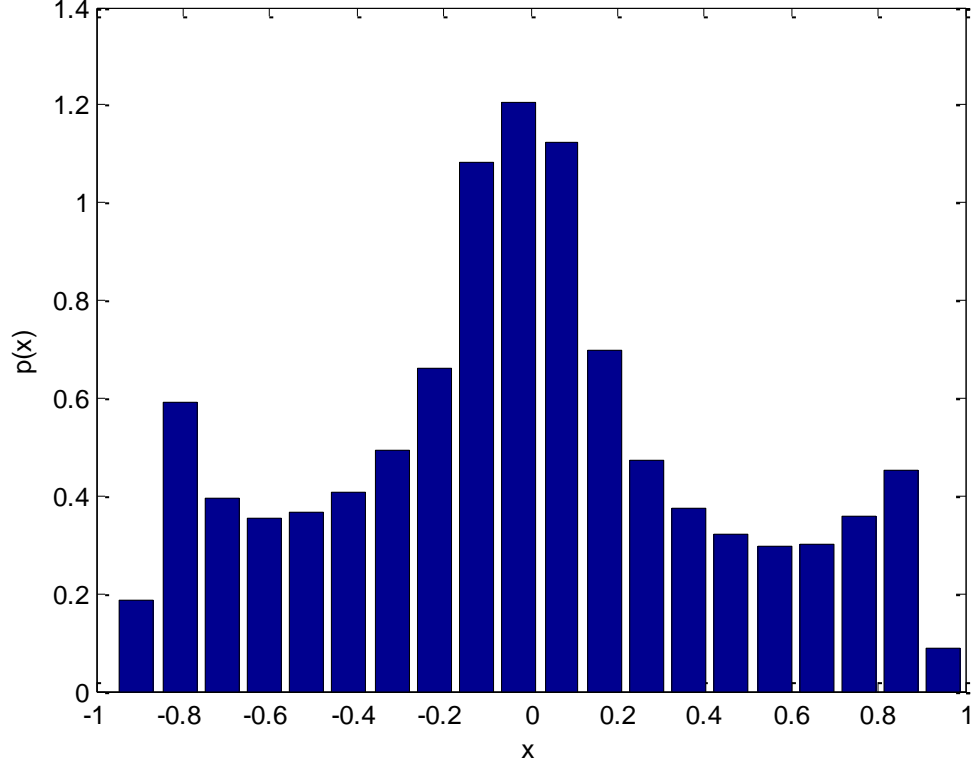


Figure 2.9: Probability density function of $x(n)$ for optimized parameter values.

2.5 Lang-Kobayashi Attractor

In order to show that the Lorenz attractor has better features such as more chaotic nature, and show the FM signal constructed from the Lorenz attractor chaotic signal has wide bandwidth and more power spectral spread we compare with the normalized Lang-Kobayashi attractor[16-17]. The mathematical expression for the dynamic normalized Lang-Kobayashi attractor is given in terms of magnitude of the state variable e , its phase φ and the state variable z as a function of normalized time variable 't' as

$$\frac{de}{dt} = ze + \eta e(t - \theta) \cos(\varphi(t) - \varphi(t - \theta) + \omega_0 \tau) \quad (2.10)$$

$$\frac{d\varphi}{dt} = Rze + \frac{\eta e(t - \theta)}{e(t)} \sin(\varphi(t) - \varphi(t - \theta) + \omega_0 \tau) \quad (2.11)$$

$$T \frac{dz}{dt} = P - z - (1 + 2z)|e|^2 \quad (2.12)$$

Where the values for $\tau = \frac{2L}{c}$, $\theta = \frac{\tau}{\tau_p}$, and other parameters are listed in Table 2 for reference.

Table 2.2: Parameter specification of the Lang-Kobayashi attractor.

Symbol	Value
η	0.02-0.09
P	1
τ	133
τ_p	4.5×10^{-12}
τ_s	700×10^{-12}
R	5
T	155.5
ω_0	2.27×10^{15}
L	0.30 meters

Figure 2.10 shows the Lang-Kobayashi attractor for control parameter values of external cavity length $L = 0.30$ meters and feedback level $\eta = 0.09$. Figure 2.11 shows the strange attractor of the Lang-Kobayashi system in different projection. Figure 2.12 shows the pseudo phase space trajectory of second projection of the Lang-Kobayashi attractor for same parameter values of external cavity length $L = 0.30$ meters and feedback level $\eta = 0.09$. Figure 2.12 illustrates that the Lang-Kobayashi attractor exhibits Diffeomorphism property showing chaotic nature of system. Figure 2.13 shows the time behavior of the Lang-Kobayashi attractor. Figure 2.14 shows the probability distribution of e for Lang-Kobayashi attractor.

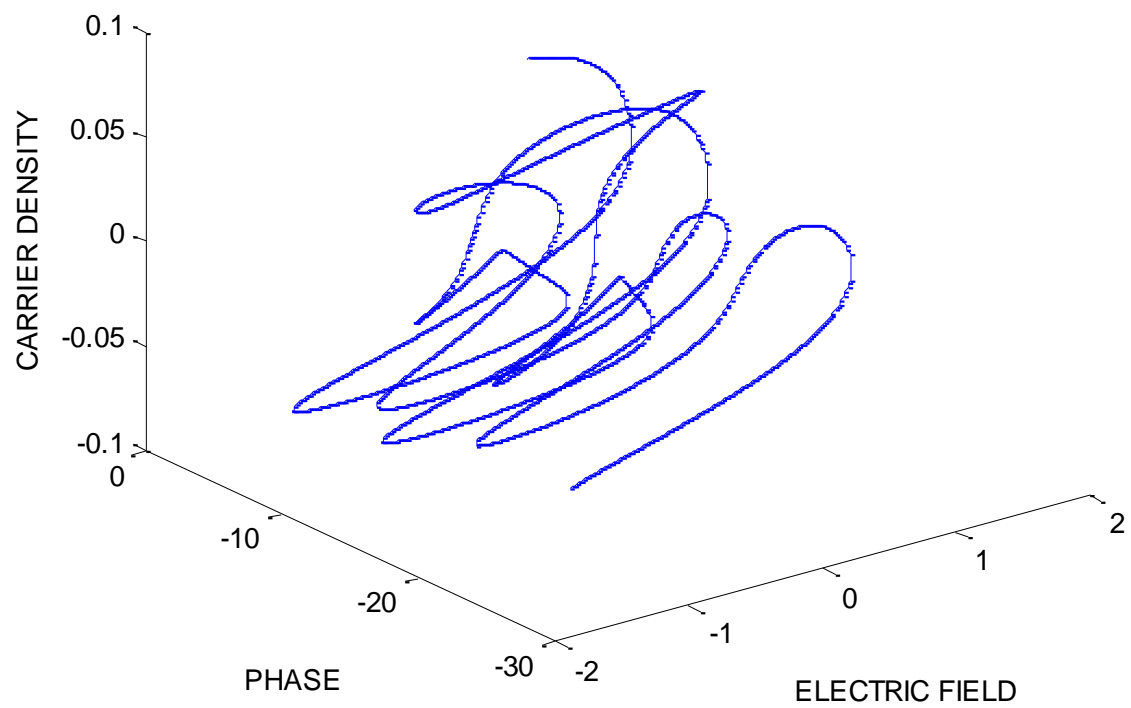


Figure 2.10: Lang-Kobayashi attractor for of $L= 0.30$ and $\eta=0.09$.

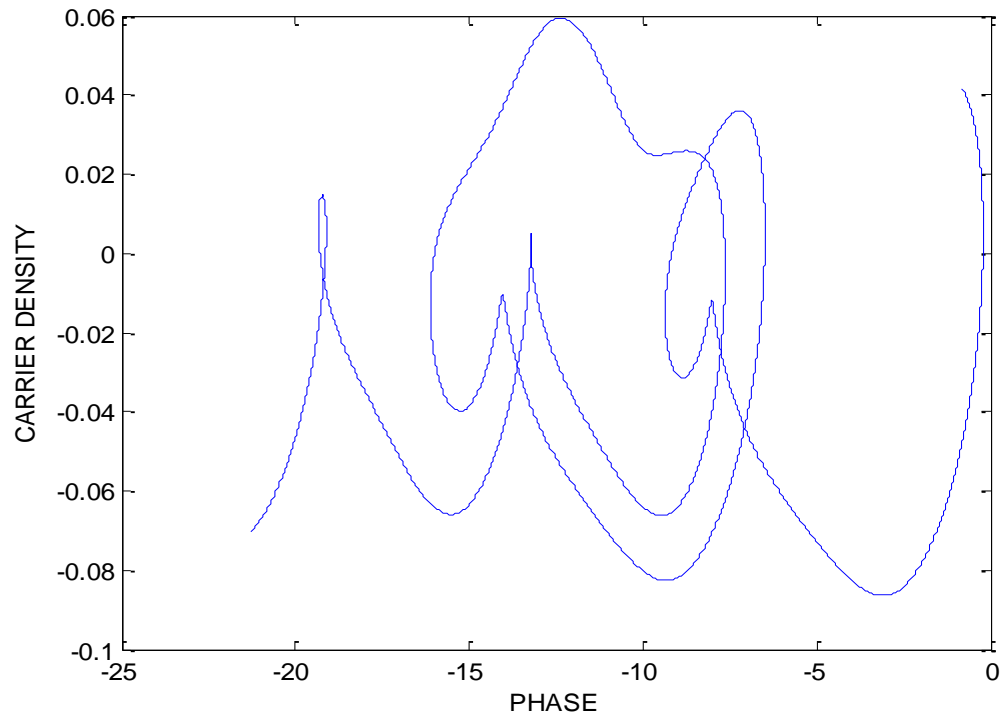


Figure 2.11: Second projection of the Lang-Kobayashi attractor.

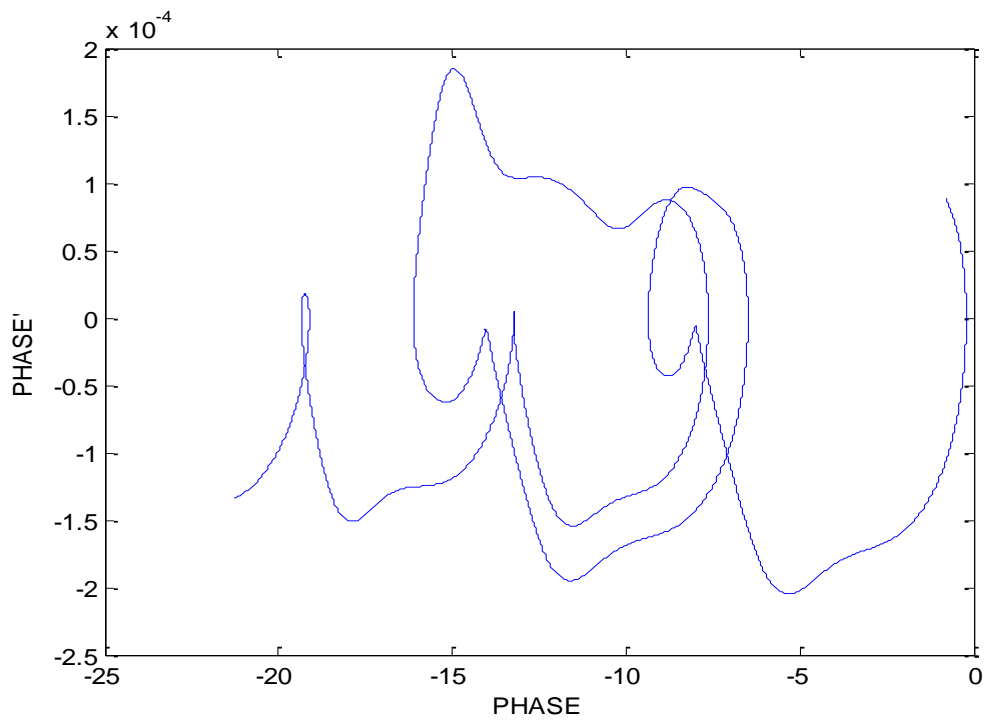


Figure 2.12: Pseudo phase space trajectory of the Lang-Kobayashi attractor.

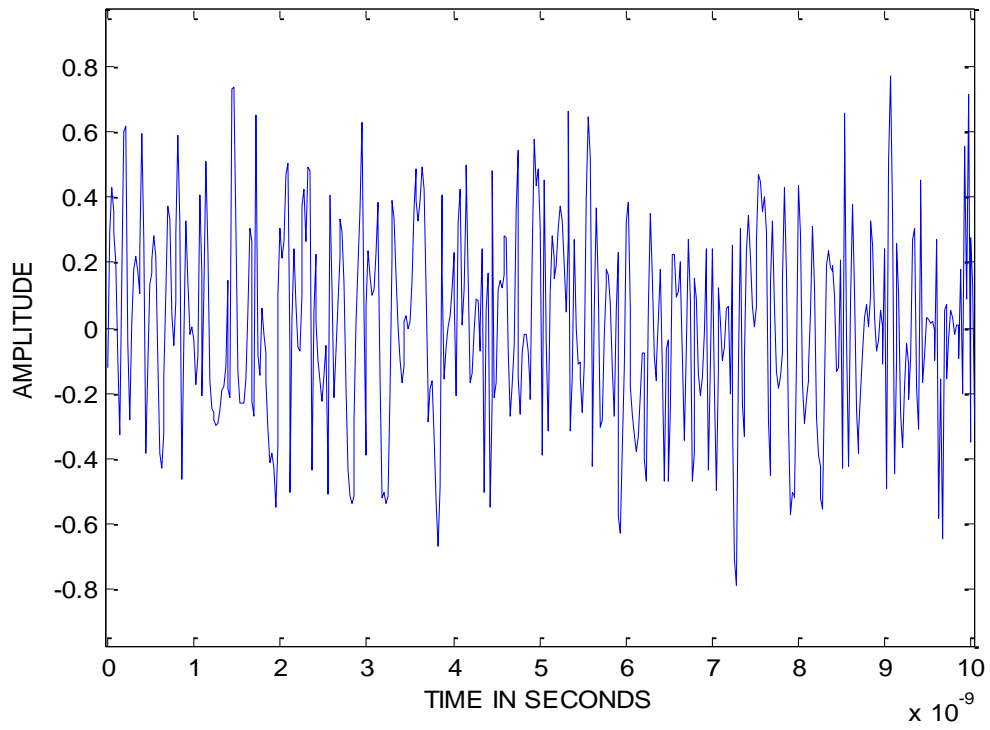


Figure 2.13: Time behavior of $e(n)$ of the Lang-Kobayashi attractor.

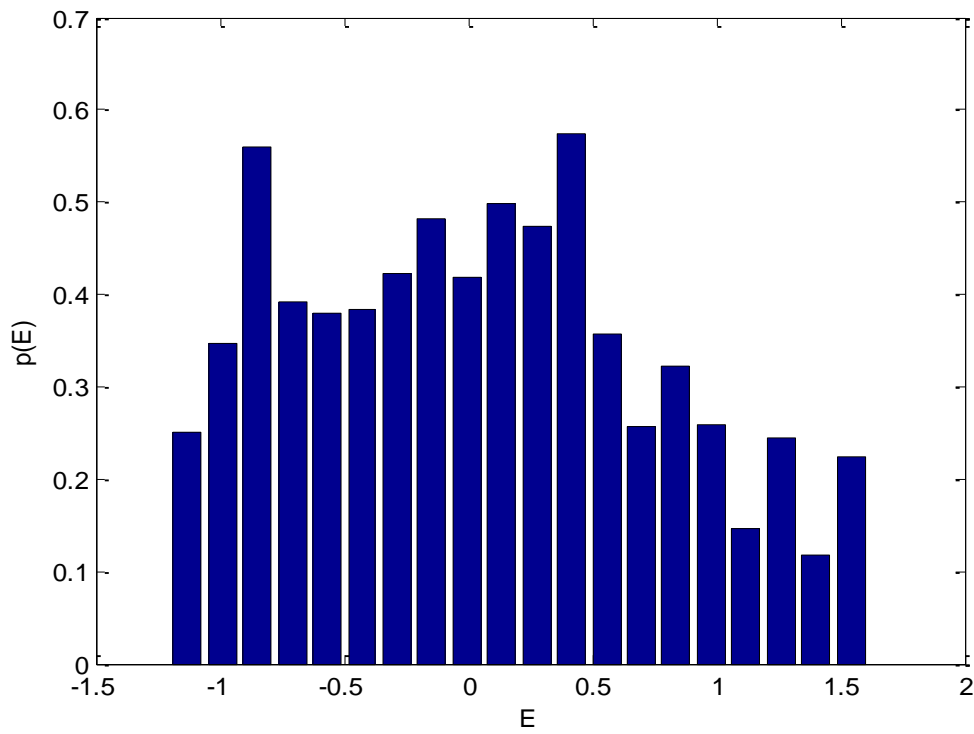


Figure 2.14: Probability density function of $e(n)$ of the Lang-Kobayashi attractor.

Chapter 3: Behavior of Chaos-Based Frequency Modulated

3.1 Frequency Modulated Signals

The frequency modulation conveys information over a carrier wave by varying its frequency.

The Frequency Modulated signal (FM signal) is given by

$$s(t) = A \cos[\theta(t)] \quad (3.1)$$

where A is the amplitude and $\theta(t)$ is the phase given by

$$\theta(t) = 2\pi f_0 t + k \int_0^t g(t') dt' \quad (3.2)$$

where f_0 is the carrier frequency, k is the modulation index and $g(t)$ is a function that conveys information. Accordingly, the instantaneous frequency is given by

$$f_i(t) = \frac{1}{2\pi} \frac{d\theta(t)}{dt} = f_0 + \frac{k}{2\pi} g(t) \quad (3.3)$$

3.2 Chaos Based Frequency Modulated Signals

Let us consider a three-dimensional Lorenz chaotic flow with variables $x(t)$, $y(t)$, and $z(t)$ as shown in equations 2.1, 2.2 and 2.3. The continuous baseband Lorenz based chaotic FM signals are given by

$$s_x(t) = A \exp[j2\pi k X(t)] \quad (3.4)$$

$$s_y(t) = A \exp[j2\pi k Y(t)] \quad (3.5)$$

$$s_z(t) = A \exp[j2\pi k Z(t)] \quad (3.6)$$

Similarly, Let us consider a three-dimensional Lang-Kobayashi chaotic flow with variables $e(t)$, $\varphi(t)$, and $z(t)$ as shown in equations 2.1, 2.2 and 2.3. The continuous baseband Lang-Kobayashi based chaotic FM signals are given by

$$s_E(t) = A \exp[j2\pi k E(t)] \quad (3.7)$$

$$s_\varphi(t) = A \exp[j2\pi k \varphi(t)] \quad (3.8)$$

$$s_Z(t) = A \exp[j2\pi k Z(t)] \quad (3.9)$$

Notice that $X(t)$, $Y(t)$ and $Z(t)$ are the corresponding time integrals of x , y , and z and $E(t)$, $\varphi(t)$, and $Z(t)$ are the corresponding time integrals of e , φ , and z of the form:

$$\Xi(t) = \sum_0^T \xi(t) \quad (3.10)$$

Depending on the FM signal, the corresponding range resolution is given by

$$\Delta r = \frac{c}{2B_\xi} \quad (3.11)$$

where c is the velocity of light and B_ξ is the bandwidth of FM signal.

The discrete version of the FM signal $s_\xi(n)$ is given by

$$s_\xi(n) = A \exp[j2\pi \Xi(n)] = A \exp[j2\pi \sum_{k=0}^n \xi(k)] \quad (3.12)$$

In order to avoid aliasing, $\Xi(n)$ is normalized with respect to twice its range

$$\Xi(n) = 2\{\max[x(n)] - \min[x(n)]\} \quad (3.13)$$

The signal $s(n)$ is ergodic in the autocorrelation if both the ensemble mean and the time mean of $s(n)s^*(n+1)$ are the same [7], i.e.

$$R(m,n) = E\{s(n)s^*(n+1)\} = \langle s(n)s^*(n+1) \rangle \quad (3.14)$$

We will show that the histogram of Real part of the FM signal $s(n)$ approaches its density regardless of whether the histogram is obtained from either a single realization of N samples or from the n th sample of an experimental ensemble. A signal is said to be wide sense stationary if

$$R(m,n) = R(m) \quad (3.15)$$

The Fourier transform of the FM signal of (3.12) is given as

$$s(f) = \int s(t) \exp^{-j2\pi ft} dt \quad (3.16)$$

By computing absolute square of (3.16) gives rise to the spectrum of the corresponding chaos based FM signal.

$$S(f) = |s(f)|^2 \quad (3.17)$$

Autocorrelation is essentially the cross correlation of the signal with itself but with zero delay. If $s(t)$ is the transmitted signal and $s(t-\tau)$ is the received signal, then autocorrelation of the signal can be given as

$$R(\tau) = E\{s(t)s(t-\tau)\} \quad (4.1)$$

The ambiguity function of the signal is used to determine the achievable range and Doppler resolution. In practice, the ambiguity function can be viewed as a time-frequency correlation of the signal that gives an idea of side lobe energy level distribution both in range-Doppler. The corresponding ambiguity surface which is the magnitude square of the ambiguity function is given by:

$$|\chi(\tau, f_d)|^2 = \left| \int s(t)s^*(t+\tau) \exp^{-j2\pi f_d t} dt \right|^2 \quad (3.18)$$

3.3 Block Diagram of Chaos Based FM Signal Generation

Figure 3.1 shows the block diagram of generation of the chaos based FM signal. The Lorenz or the Lang-Kobayashi oscillator develops the chaotic signal which is used as input to the voltage control oscillator. FM signal is fed to the band pass filter and a certain part of FM signal is leaked to the Correlator which acts as a reference signal. From the band pass filter the signal is delivered to Phased array blocks by means of waveguide or other transmission lines, which is used as antenna for the purpose of the signal transmission. Using phase shifters at each of radiating elements, an electronically driven phase arrays can rapidly change the direction of antenna beam in space without moving antenna manually. Mixing the received signal with reference signal and using low pass filter gives a low frequency component signal which is the input for display and a decision is made whether target is present or not. The radars vary the frequency of transmitted signal and measure the range based on instantaneous transmitted and received signals. Whenever there is shift in the Doppler the radial velocity of the target can be found.

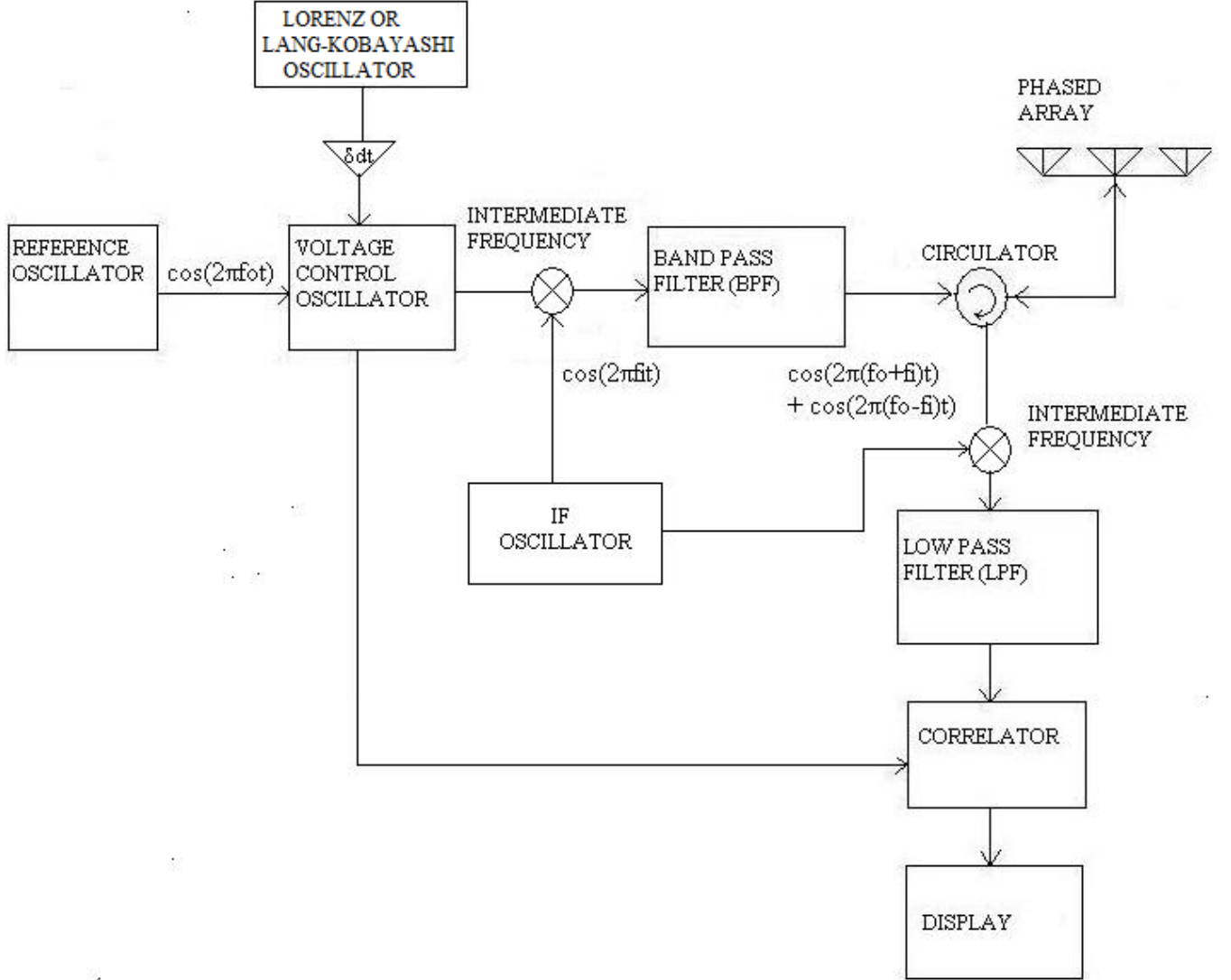


Figure 3.1: Block diagram of the Chaos based FM signal generation.

3.4 Ergodicity, Time-Frequency Analysis and Spectra

We chose any one of the state variables x , y or z as instantaneous frequency to generate realizations of the wideband Lorenz chaotic FM signal $s(n)$. Similarly we choose any one of the state variables E , φ or Z as instantaneous frequency to generate realizations of the wideband Lang-Kobayashi chaotic FM signal $s(n)$. Figure 3.2 shows that the constructed Lorenz chaotic FM signal $s(n)$ is the same for the ensemble mean [9] and the time mean of $s(n)s^*(n+1)$ in normal parameter space region. Figure

3.3 shows that the constructed FM signal $s(n)$ is the ergodic in highly chaotic parameter space region. Similarly, Figure 3.4 shows that the Lang-Kobayashi chaotic FM signal $s(n)$ is the same for the ensemble mean [9] and the time mean of $s(n)s^*(n+1)$. Plots with '*' are obtained by processing 1024 samples of a single realization. The plots with ' Δ ' are obtained from the 1024th sample of the 1024 realizations of $s(n)$ with an arbitrary initial condition. The ergodicity in the mean of $s(n)$ is apparent from the provided illustration [10].

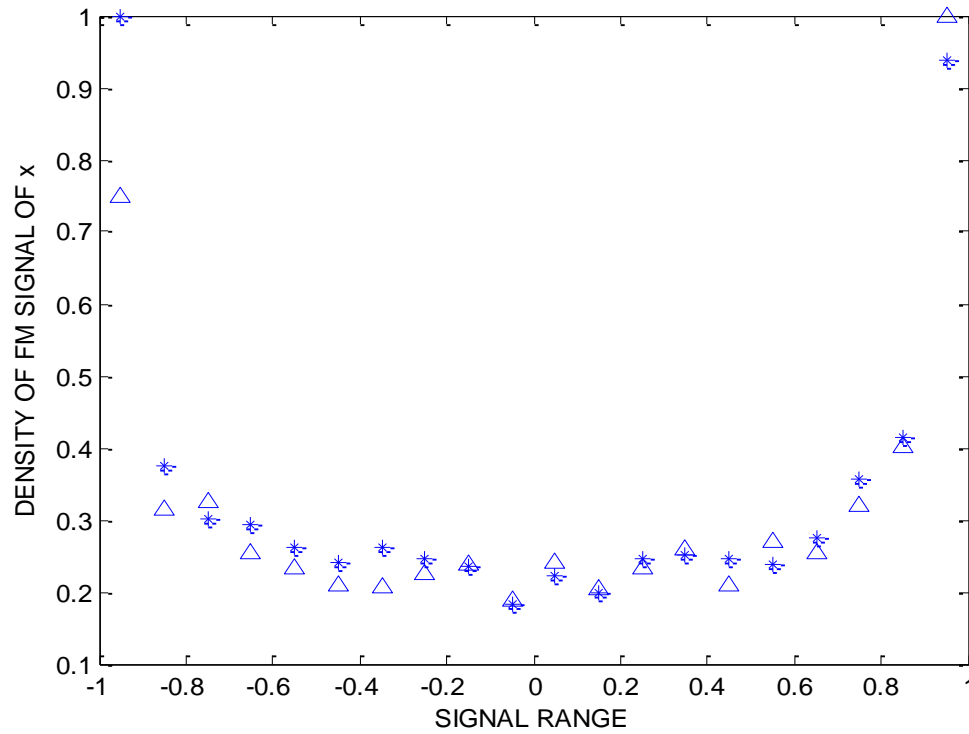


Figure 3.2: Ergodic behavior of the Lorenz chaotic FM signal for reference parameter values.

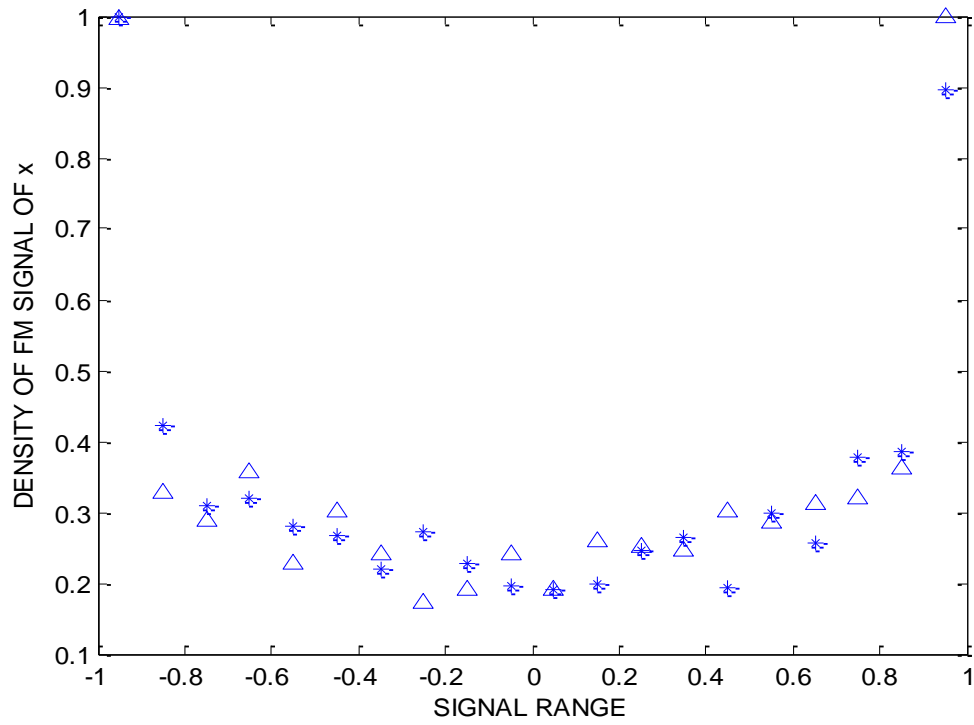


Figure 3.3: Ergodic behavior of the Lorenz chaotic FM signal for optimized parameter values.

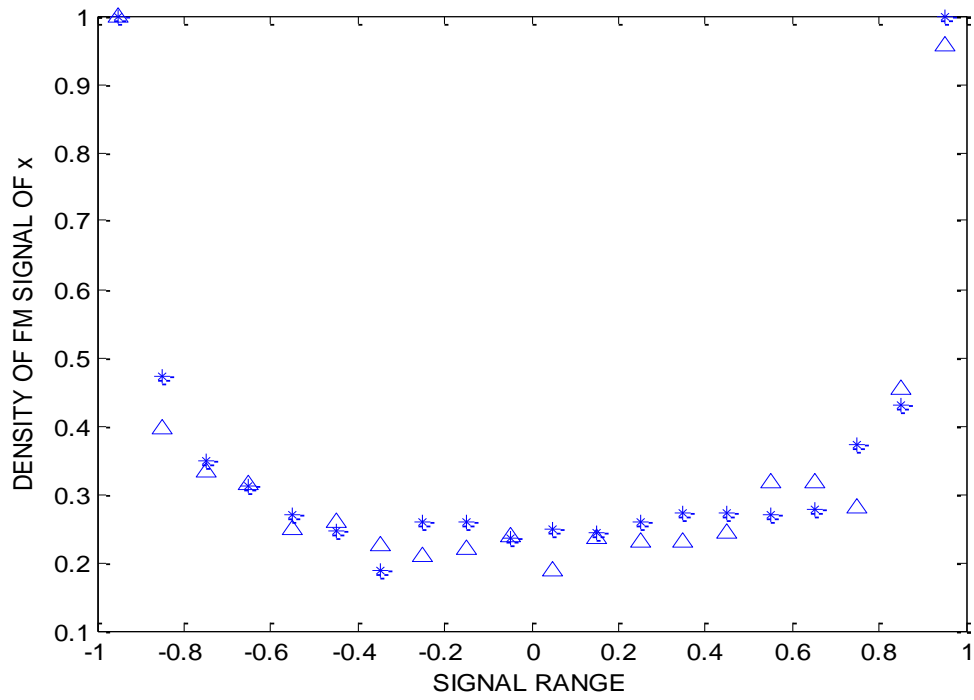


Figure 3.4: Ergodic behavior of the Lang-Kobayashi chaotic FM signal.

The pseudo-phase space trajectories [11] of constructed FM signals obtain the shape as a strange attractor. The strange attractor may take on the shape of a Mobius strip, disc or extended disc based on the time evolution of the signal. The time-frequency distribution of the FM signal is characterized by taking the entire signal into several frames of $L=4500$ of length $M=4096$ samples each frame. A time-frequency distribution has a wideband centered on a time shifting carrier frequency. This carrier frequency continuously shifts in a linear or quadratic pattern over a range of $(0, f_s)$, and the pattern on a time-frequency distribution appears to be fractal in nature, same as a chaotic signal. Two comparisons are made based on the time evolution of the pseudo-phase space trajectory of the FM signal, its spectrum and its time frequency analysis.

In the first case, the pattern on a time-frequency distribution exhibits fractals in a linear or a quadratic pattern. Whenever a time-frequency distribution has a linear pattern the corresponding pseudo-phase space trajectory of the FM signal appears as a Mobius strip. The spectrum of the corresponding FM signal, whose pseudo-phase space attractor takes shape as a Mobius strip, has a wide bandwidth with broad band characteristics. If a time-frequency distribution has a quadratic pattern, its corresponding pseudo-phase space trajectory of the FM signal appears as an extended disc and the respective spectrum has very narrow bandwidth. In between the linear and quadratic pattern of a time-frequency distribution the pseudo-phase space trajectory of the FM signal appears as a circular disc with the spectrum having narrow bandwidth. Figure 3.5 and Figure 3.6 shows the fragment of a time-frequency distribution and behavior of the corresponding pseudo-phase space trajectory and its spectrum depending on the time evolution of the Lorenz chaotic FM signal and the Lang-Kobayashi chaotic FM signal respectively.

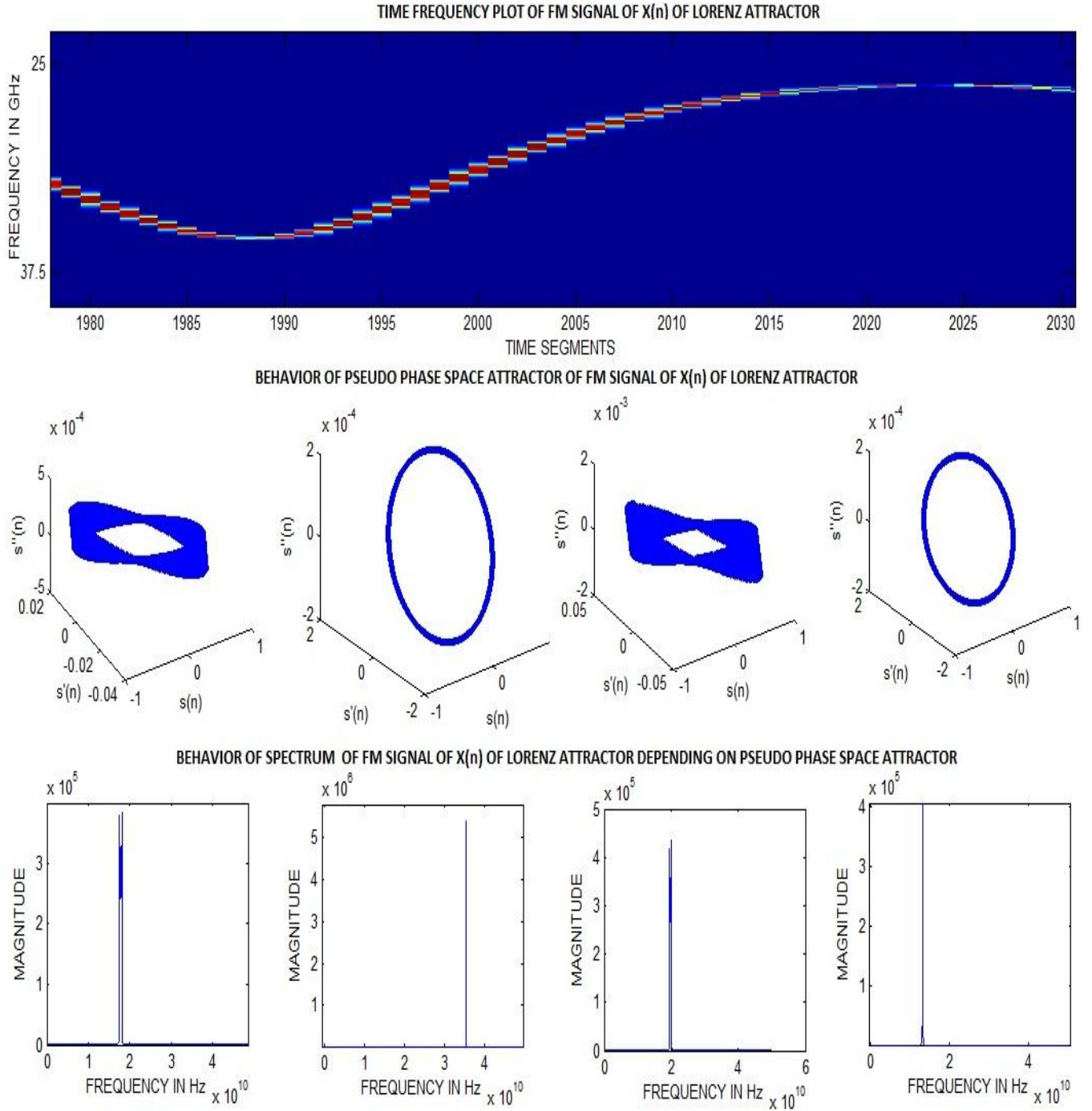


Figure 3.5: Behavior of pseudo phase space trajectory and spectrum of the Lorenz chaotic FM signal depending on time-frequency distribution.

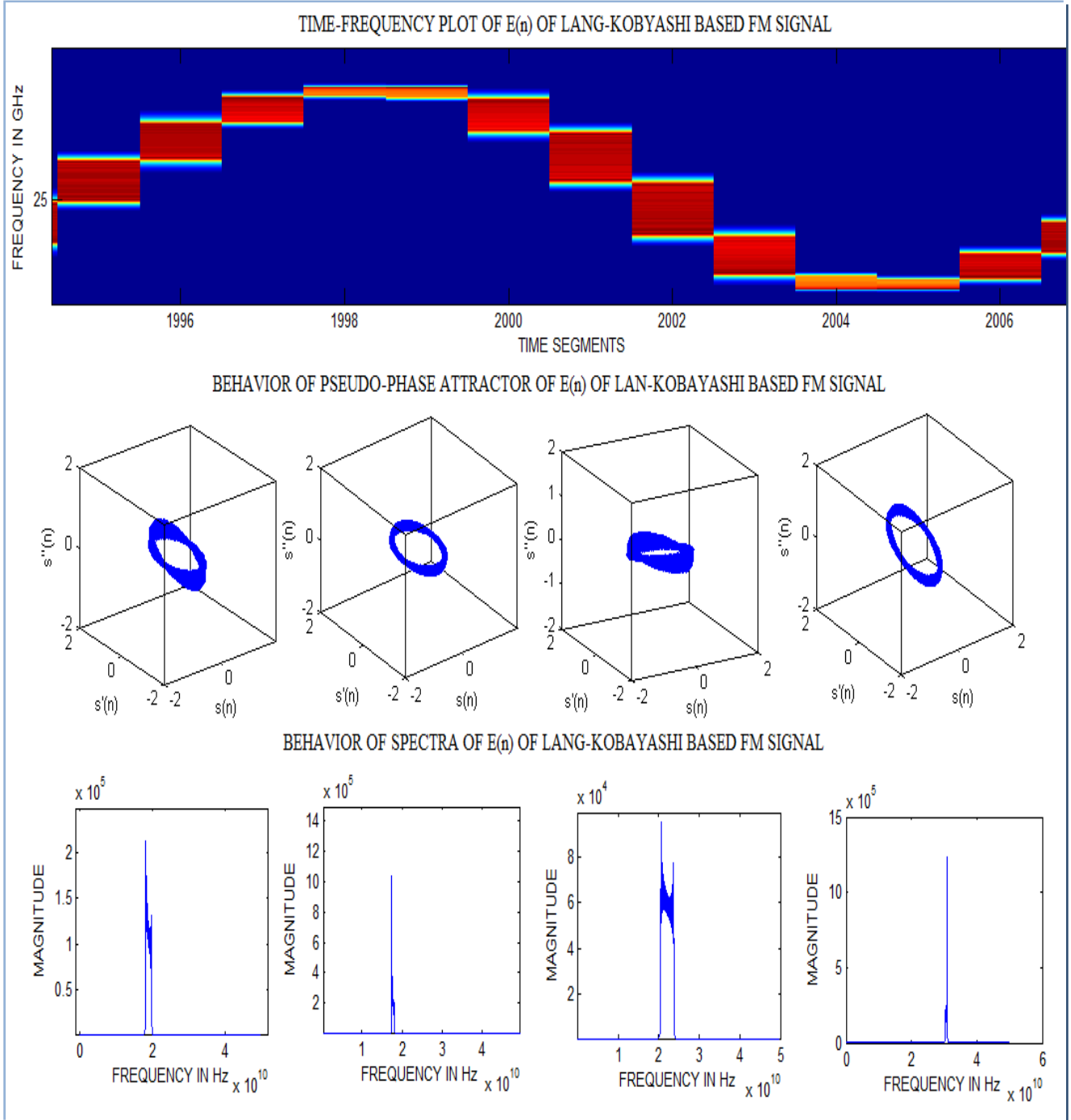


Figure 3.6: Behavior of pseudo phase space trajectory and spectrum of the Lang-Kobayashi chaotic FM signal depending on time-frequency distribution.

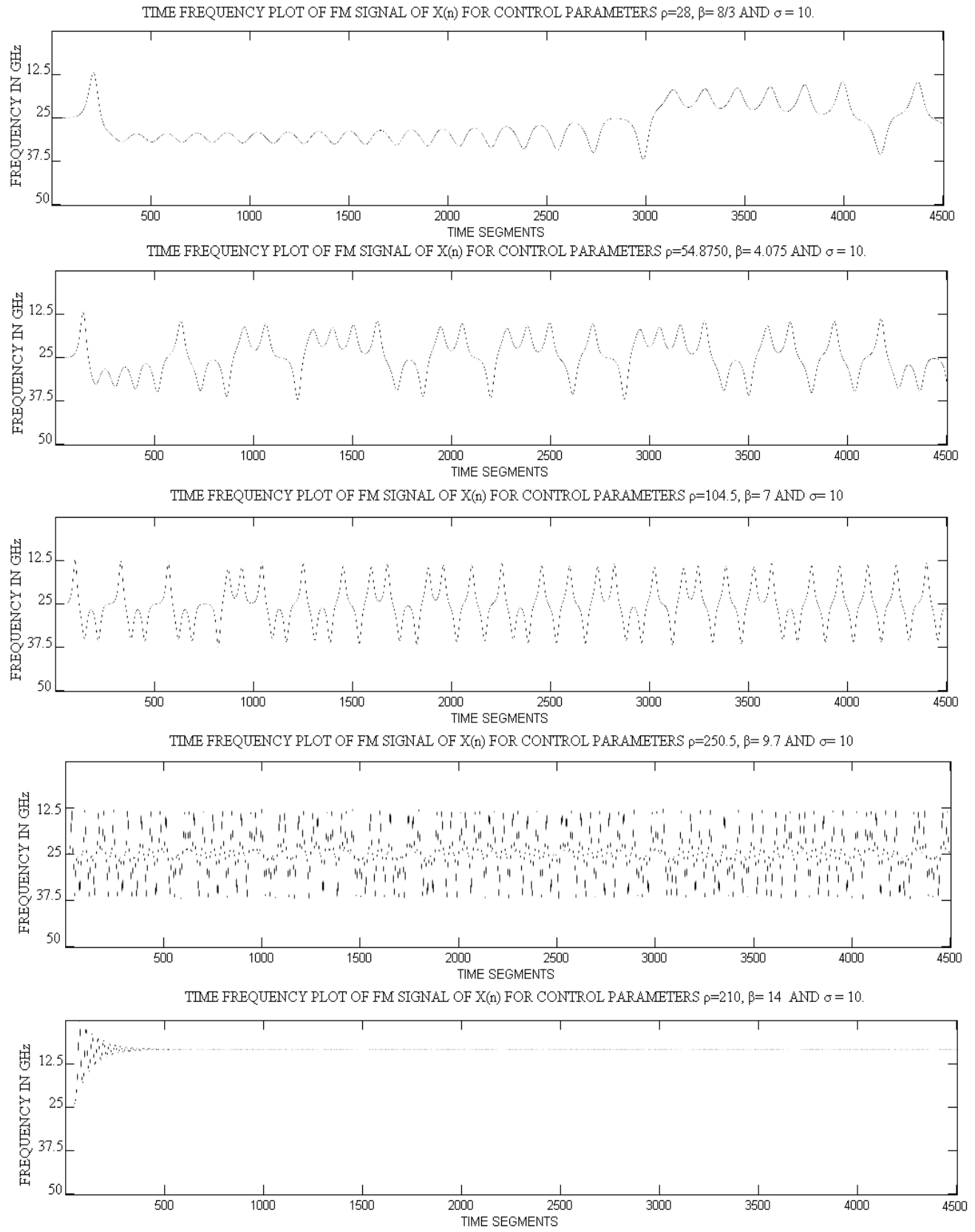


Figure 3.7: Time-frequency distribution analysis of the Lorenz chaotic FM signals in different parameter space regions.

In the second case, as shown in Figure 3.7, a time-frequency distribution behavior of the FM signal is simulated in different chaotic regions. Keeping σ constant as 10, a time-frequency analysis of the FM signal at ρ equal to 28.00 and β equal to 2.67 has less fractal in nature. Similarly, a time-frequency analysis of the FM signal at ρ equal to 55.42 and β equal to 4.01 has better fractal nature. As mentioned above, in the optimal region the FM signal behaves optimally and its time-frequency analysis has more fractal behavior. Just above the highly chaotic parameter space region, the Lorenz chaotic signal behaves as a transient chaos. A Time-Frequency Analysis of the FM signal constructed in this region resembles its chaotic signal having transient fractal behavior.

Figure 3.8 shows the complete time-frequency distribution of the FM signal of $x(n)$ for highly chaotic parameter space region with values of β equal to 9.00, ρ equal to 172.00 and σ equal to 10.00. Figure 3.9 shows the close up view of time-frequency distribution of the FM signal of $x(n)$ for parameter value of β equal to 9.00, ρ equal to 172.00 and σ equal to 10.00. Figure 3.10 shows the complete time-frequency distribution of the FM signal of $E(n)$ parameter values of L equal to .30 and η equal to 0.09 while Figure 3.11 shows the close up view of time-frequency distribution of the FM signal of $E(n)$ for same parameter values.

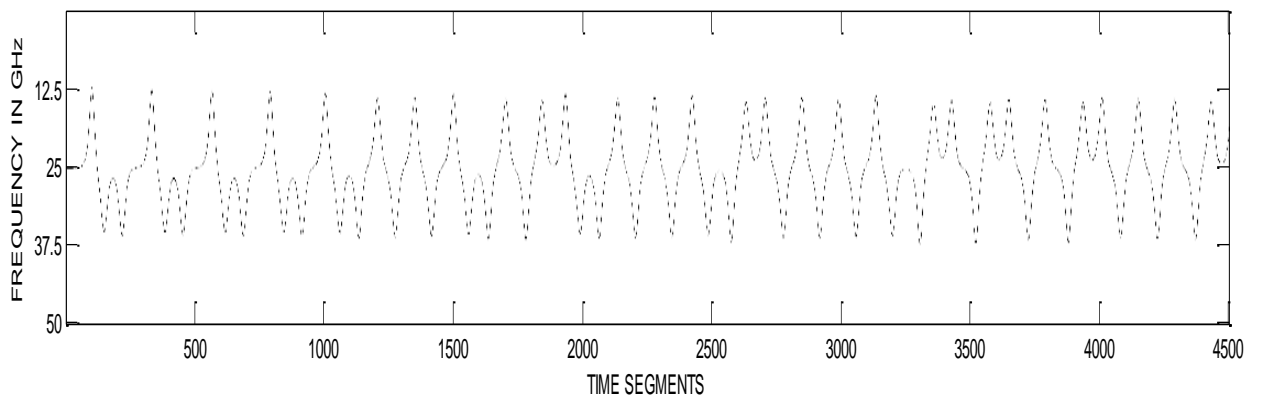


Figure 3.8: Time-frequency distribution of the Lorenz chaotic FM signal for optimized Parameter values.

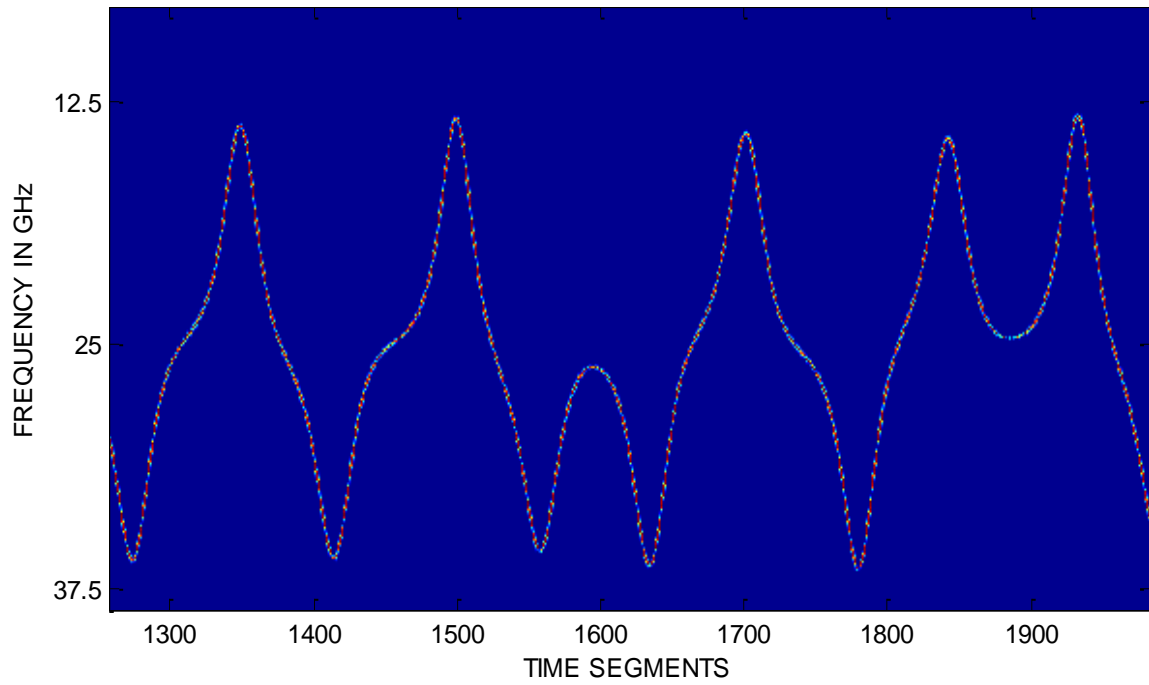


Figure 3.9: Close up view of time-frequency distribution of the Lorenz chaotic FM signal for optimized parameter values.

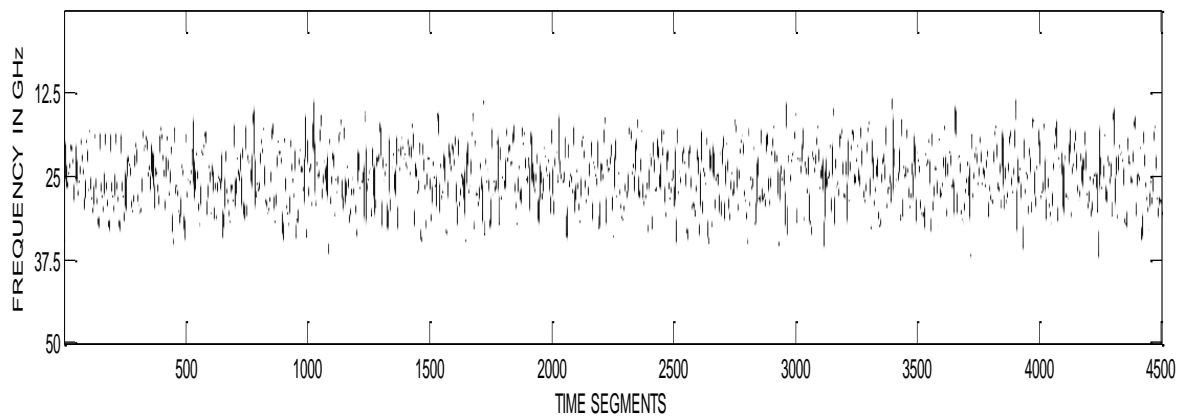


Figure 3.10: Time-frequency distribution of the Lang-Kobayashi chaotic FM signal.

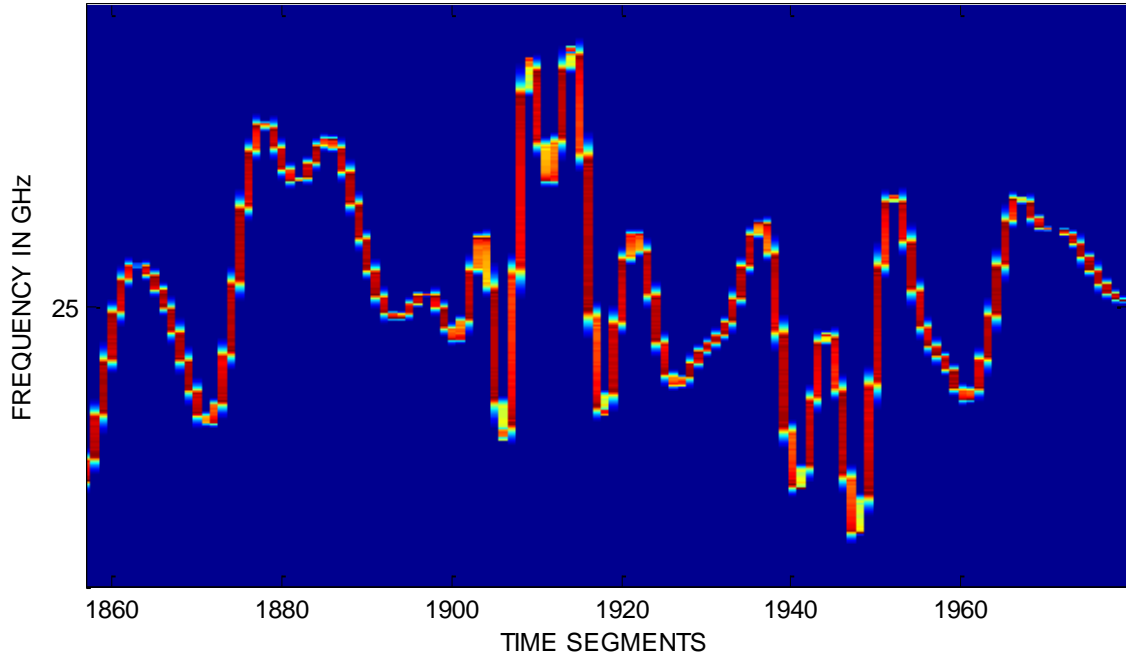


Figure 3.11: Close up view of time-frequency distribution of the Lang-Kobayashi chaotic FM signal.

Depending on the slope of a time-frequency distribution, a finite number of discrete wide bandwidths with in-ultra high wide bandwidth are achieved. This method is known as frequency agility which can be used to detect targets even in presence of jammer. Using this type of technique it is easy to achieve required range of frequencies to obtain high resolution and reduce glint error [12]. Since the bandwidth obtained for different instants of time varies in range of 150MHz it is easy to decorrelate the glint error.

3.5 Bandwidth Improvement Based on Time-Frequency Distribution

From Figure 3.8 and Figure 3.10, we consider the entire FM signal that gives corresponding positive linear pattern of time-frequency distribution as N. The pseudo phase space trajectory of the FM signal that has positive linear pattern appears as a Mobius strip. The area of Mobius strip depends on the value and length of the slope. The spectrum possesses wide bandwidth depending on the slope and length of linear pattern on time-frequency distribution. As length increases and the slope of linear

pattern tends to unity we get Mobius strip of large area, with many orbits and corresponding spectrum has wide band in nature as shown in Figure 3.12 and Figure 3.13.

Since the time-frequency distribution of the Lorenz attractor at normal parameter space region has less fractal behavior as shown in Figure 3.7, the corresponding linear patterns has less length and slope. Hence the spectrum has narrow bandwidth.

The time-frequency distribution of the Lorenz attractor at highly chaotic parameter space region has more fractal behavior as shown in Figure 3.7, the corresponding linear patterns has more length and slope. Hence the spectrum has wide bandwidth as shown in Figure 3.14 compared to that of spectrum of the FM signal constructed in normal parameter space region.

Similar results are obtained for the Lang-Kobayashi attractor whose time-frequency distribution more fractal behavior as shown in Figure 3.10, the corresponding linear patterns has more length and slope. Hence the spectrum has wide bandwidth as shown in Figure 3.15.

Since the time-frequency distribution of the Lorenz chaotic FM signal has more length and slope of linear pattern, the corresponding FM signal has more power spectral spread compared to the Lang-Kobayashi chaotic FM signal. This can be illustrated in Figure 3.14 and 3.15 where the Lorenz chaotic FM signal has more power spectral spread.

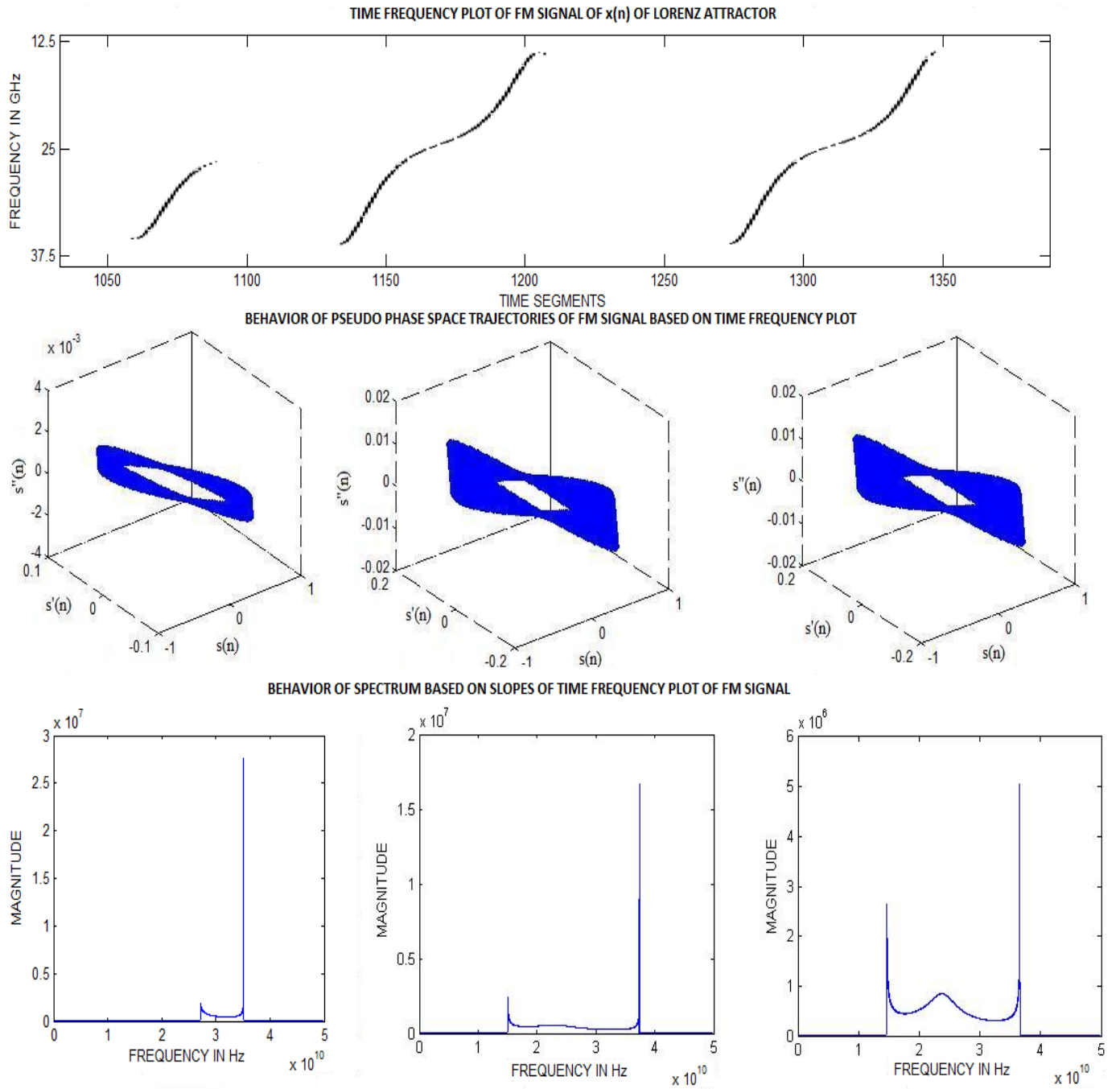


Figure 3.12: Behavior of pseudo phase space trajectory and spectrum of the Lorenz FM signal depending on slope and length of time-frequency distribution of FM signal.

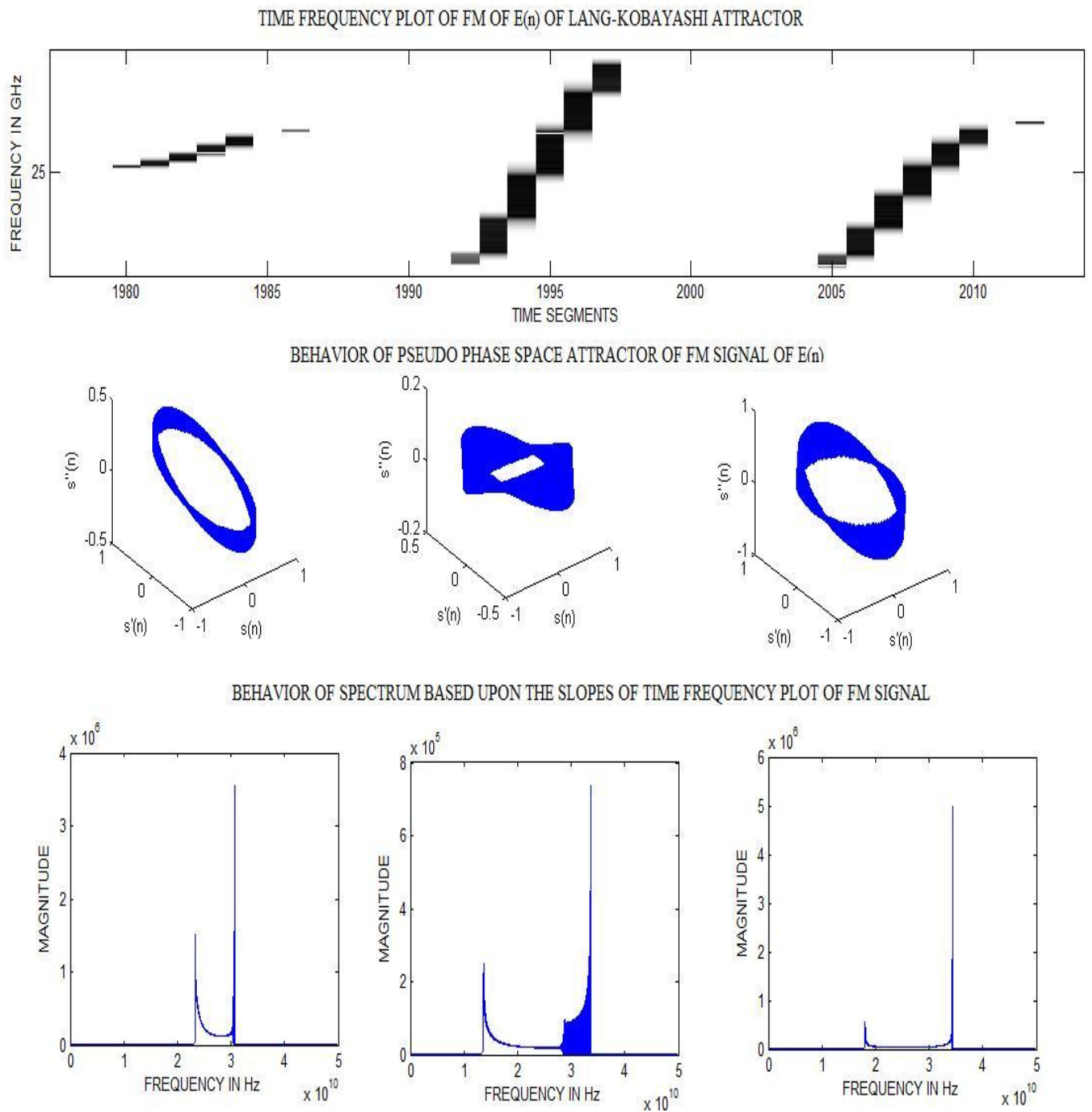


Figure 3.13: Behavior of pseudo phase space trajectory and spectrum of the Lang-Kobayashi FM signal depending on slope and length of time-frequency distribution of FM signal.

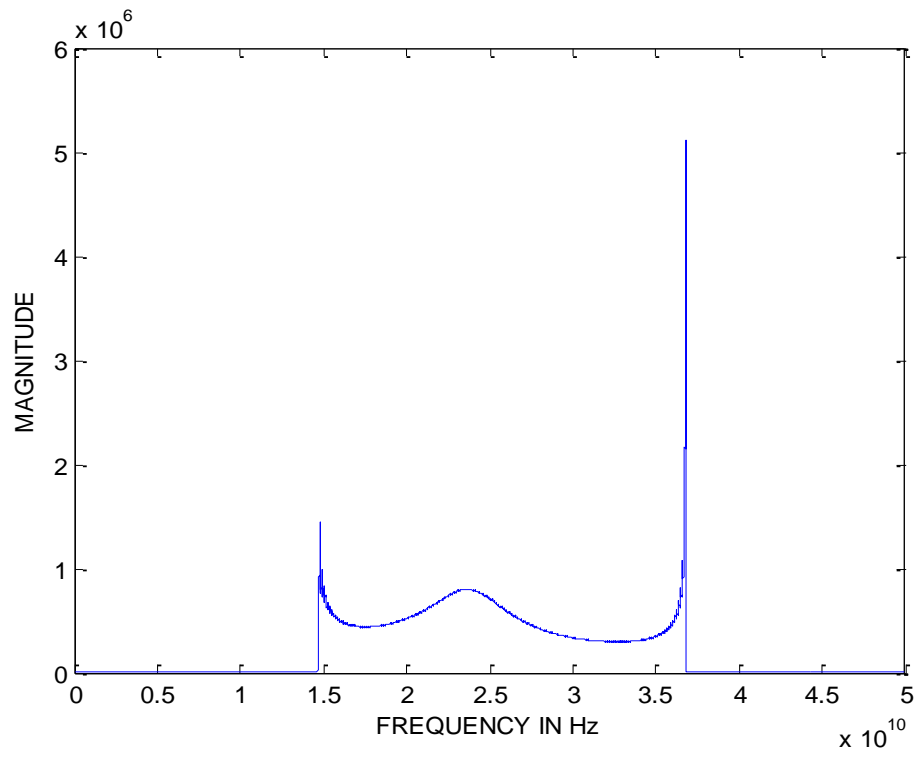


Figure 3.14: Spectral behavior of the Lorenz chaotic FM signal for optimized parameter.

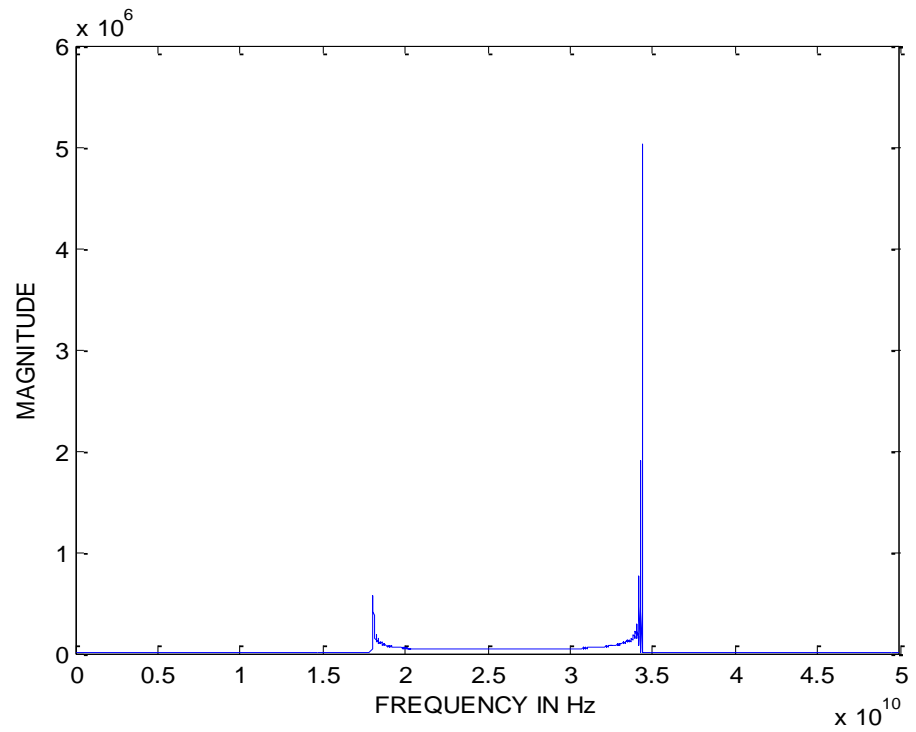


Figure 3.15: Spectral behavior of the Lang-Kobayashi chaotic FM signal.

Chapter 4: Statistical Analysis of Chaos-Based Frequency Modulated Signals

4.1 Time Bandwidth Product of Chaos Based Frequency Modulated Signals

One of the main issues in detecting the target is optimizing time-bandwidth product. Range resolution for given radar can be significantly improved using very short pulses. However utilizing short pulses decrease the average transmitting power, which can hinder radar's normal modes of operation, particularly for multi-function and surveillance radars. Thus pulse width of transmitted signal should be increased simultaneously maintaining adequate range resolution. Therefore it is always tradeoff in choosing the duration of single pulse to be transmitted in order to achieve high resolution in range and Doppler. This can be resolved by using pulse compression techniques which depends on time-bandwidth product of transmitted signal. Hence time-bandwidth product improvement is always challenging and desirable feature required for signal to be transmitted.

Figure 4.1 shows the results obtained for the range of time-bandwidth product for the reference Lorenz chaotic FM signal. The time-bandwidth product in this case is typically around 50,000. Figure 4.2 shows the results obtained for the range of time-bandwidth product for the optimized FM signal. The time-bandwidth product exceeds 75,000 in this case. Similarly, Figure 4.3 shows the time-bandwidth product for the Lang-Kobayashi chaotic FM signal. The range of time-bandwidth products obtained in this case is around 50,000. Hence the compression gain or signal to noise optimization or matched filter gain is high for the optimized Lorenz chaotic FM signal using a right choice for signal transmission.

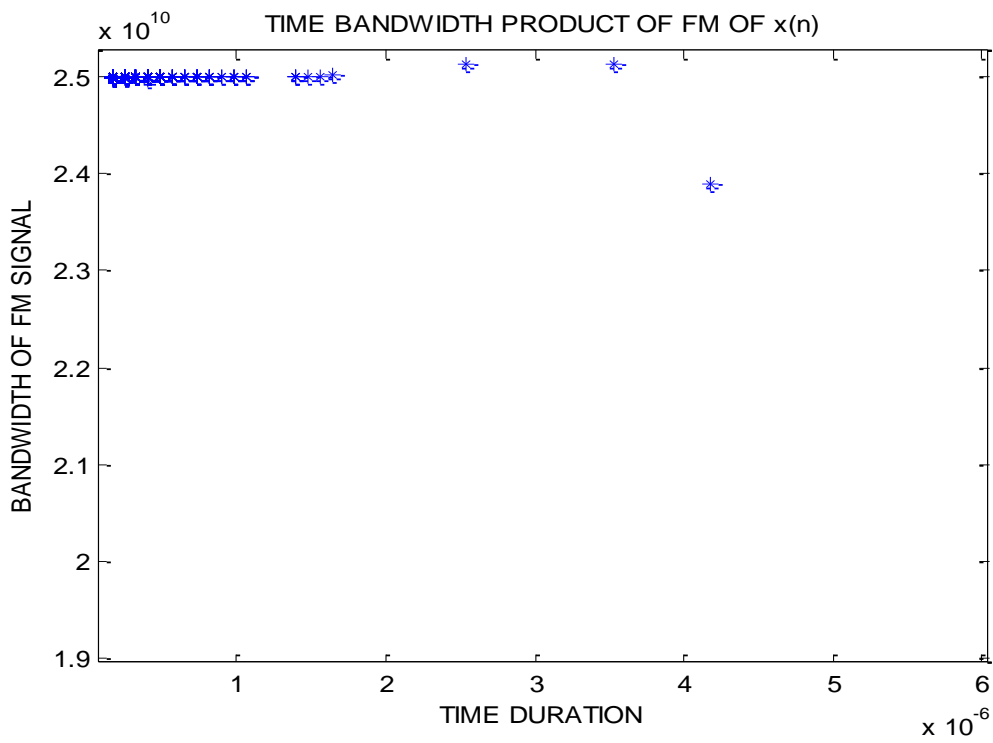


Figure 4.1: Time-bandwidth product of the Lorenz chaotic FM signal for reference parameter values.

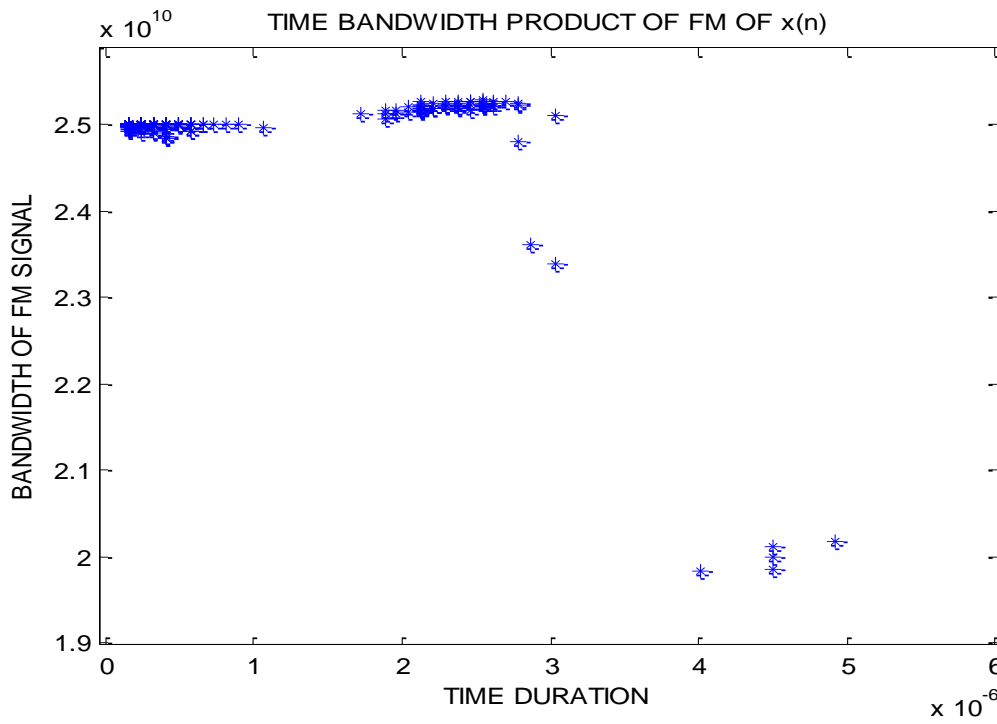


Figure 4.2: Time-bandwidth product of the Lorenz chaotic FM signal for optimized parameter values.

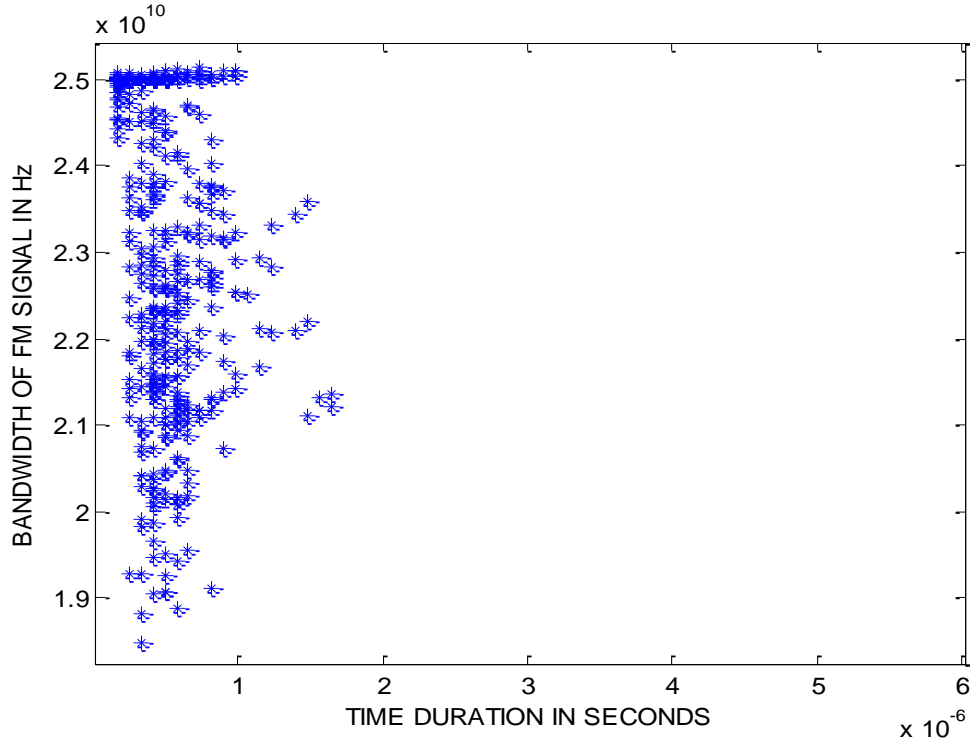


Figure 4.3: Time-bandwidth Product of the Lang-Kobayashi chaotic FM signal.

4.2 Fractional Bandwidth of Chaos Based Frequency Modulated Signals

A rule of thumb for a signal to be wideband is that its fractional bandwidth β_0 should be greater than 0.1. The fractional bandwidth of a signal is a measure how wideband the signal is. If the signal has center frequency f_c between lower frequency f_1 and higher frequency f_2 then fractional bandwidth can be given as

$$\beta_0 = \frac{f_2 - f_1}{f_c} = \frac{2(f_2 - f_1)}{f_2 + f_1} \quad (2.4)$$

Clearly fractional bandwidth varies from minimum value of zero to maximum value of 2. The higher the fractional bandwidth value the wider the bandwidth of signal is.

Figure 4.4 shows the results obtained for the range of fractional bandwidth of the reference Lorenz chaotic FM signal. Figure 4.5 shows the fractional bandwidth for the optimized Lorenz chaotic FM signal. Figure 4.6 shows the result obtained for the Lang-Kobayashi chaotic FM signal. It is obvious from the illustrated results that all the signals are exhibiting wideband characteristics. In particular most of the reference Lorenz chaotic local FM signals has fractional bandwidth of 0.8 but most of the optimized Lorenz chaotic local FM signal has fractional bandwidth of 1. In case of the Lang-Kobayashi chaotic local FM signal the fractional bandwidth is of range 0.9 to 1. Since the signal has more fractional bandwidth, it possesses a wideband characteristic nature which gives range resolution of radar less than a few meters.

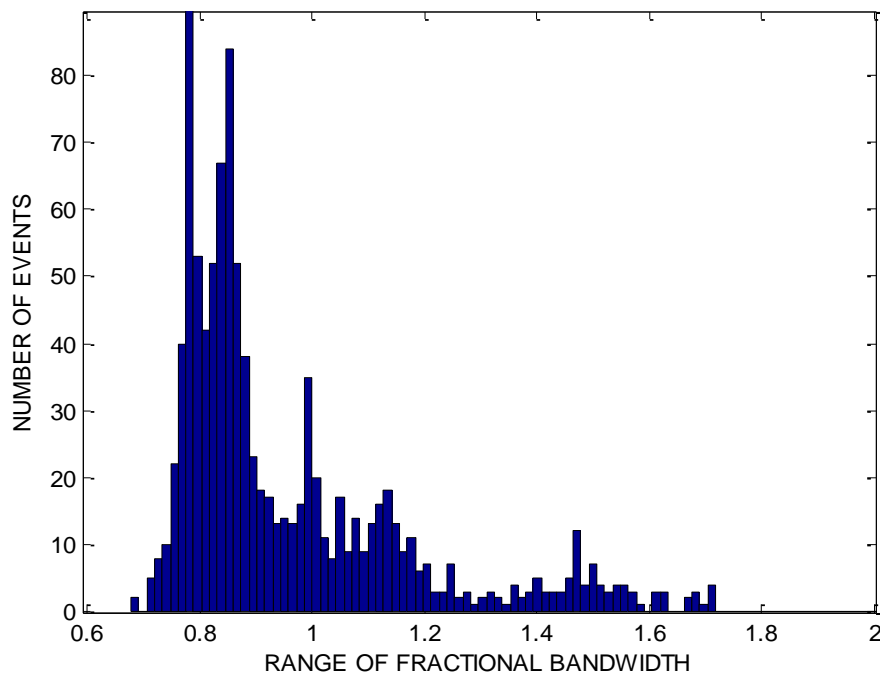


Figure 4.4: Range of fractional bandwidth of the Lorenz chaotic FM signal for reference parameter values.

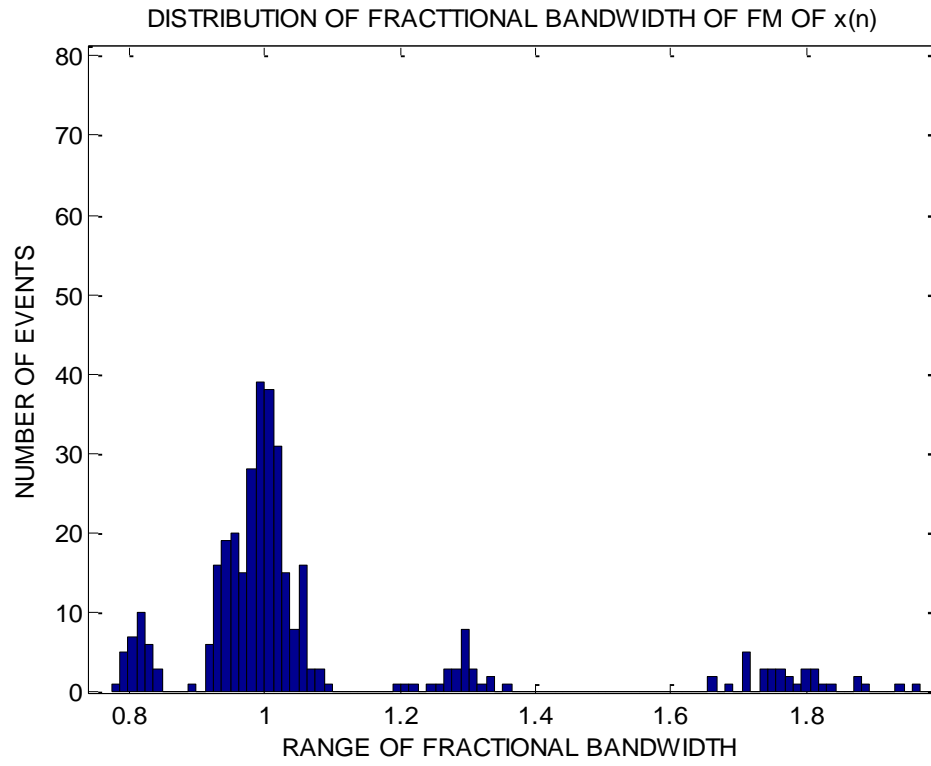


Figure 4.5: Range of fractional bandwidth of the Lorenz chaotic FM signal for optimized parameter values.

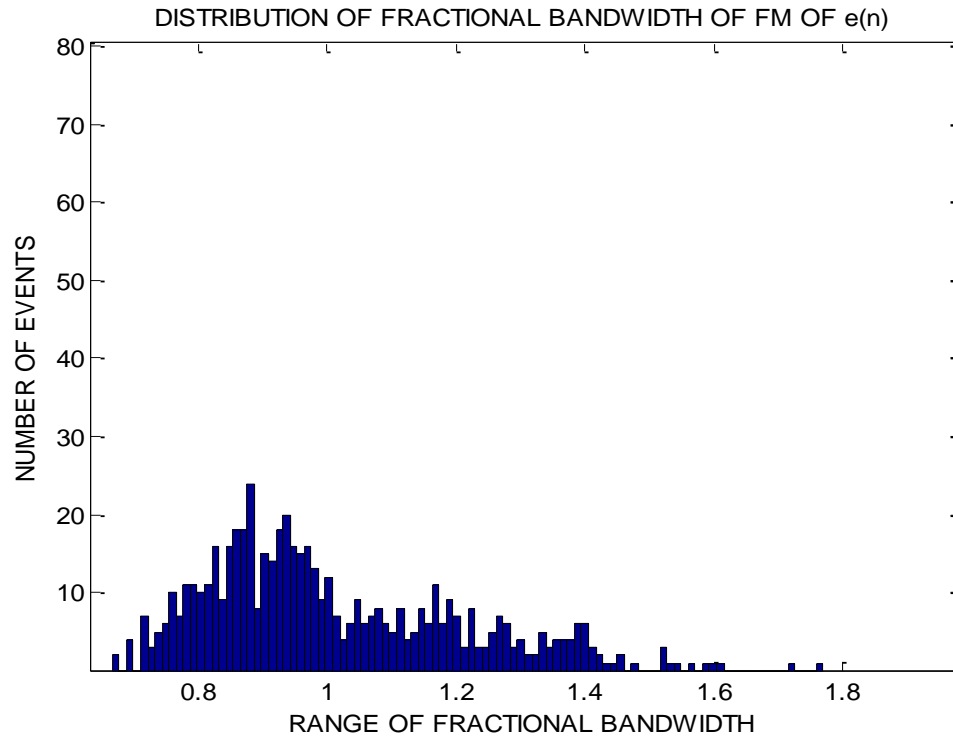


Figure 4.6: Range of fractional bandwidth of the Lang-Kobayashi chaotic FM signal.

Radar jamming refers to radio frequency signals originating from sources outside the radar, transmitting in radar's frequency and thereby masking targets of interest. The originating of foreign signals can be done by operating at same center frequency. Apart from transmitting same frequency signals during some occasions there might be chance of blocking the radar transmitting signals. In order to avoid all the above problems electronic counter countermeasure for persistence of anti-jamming and collision warning is necessary. Such can be made possible by achieving frequency agility of a signal where a finite number of discrete wide bandwidths with in-ultra high wide bandwidth are achieved. Hence there will be always a center frequency varying depending on each discrete wideband.

Hence the varied center frequency can be estimated by plotting its distribution. Figure 4.7 shows the center frequency distribution for the reference Lorenz chaotic FM signal. Figure 4.85 shows the center frequency distribution for the optimized Lorenz chaotic FM signal. Figure 4.9 shows the result obtained for the center frequency distribution of the Lang-Kobayashi chaotic FM signal. It is obvious that the center frequency distribution of the Lang-Kobayashi chaotic FM signal range making it a good choice for transmission of signal during the presence of jammer.

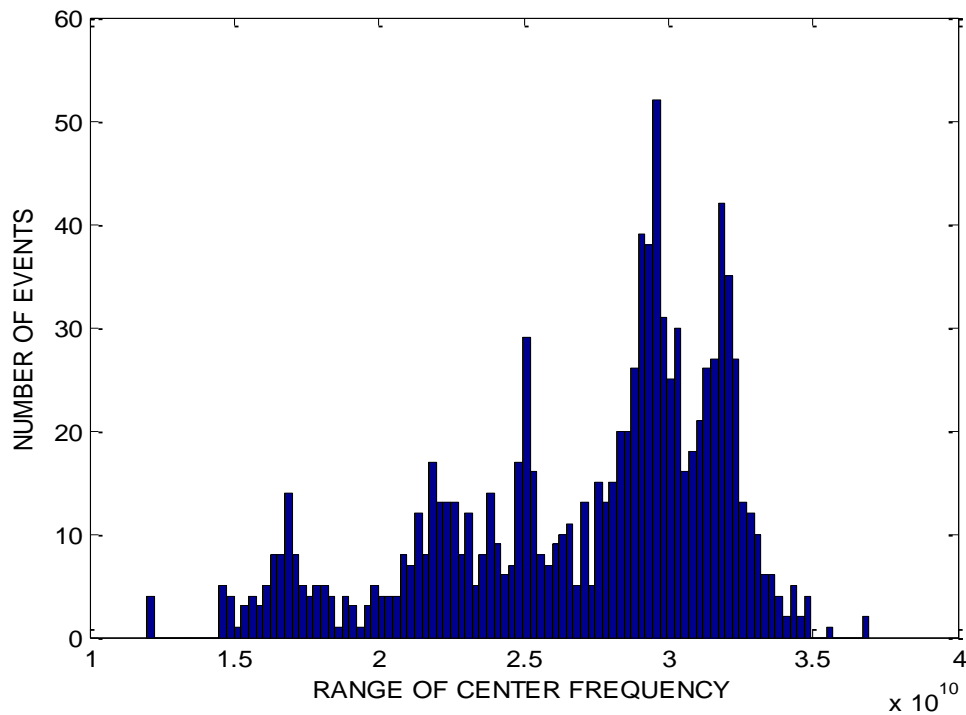


Figure 4.7: Distribution of center frequency of the Lorenz chaotic FM signal for reference parameter values.

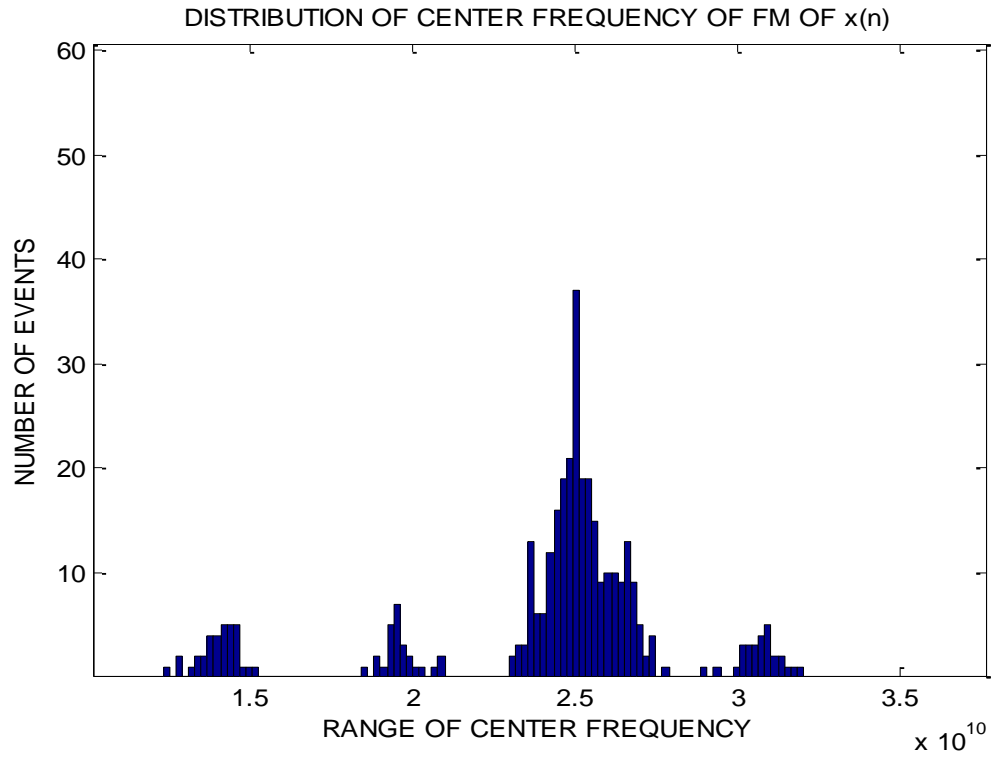


Figure 4.8: Distribution of center frequency of the Lorenz chaotic FM signal for optimized parameter values.

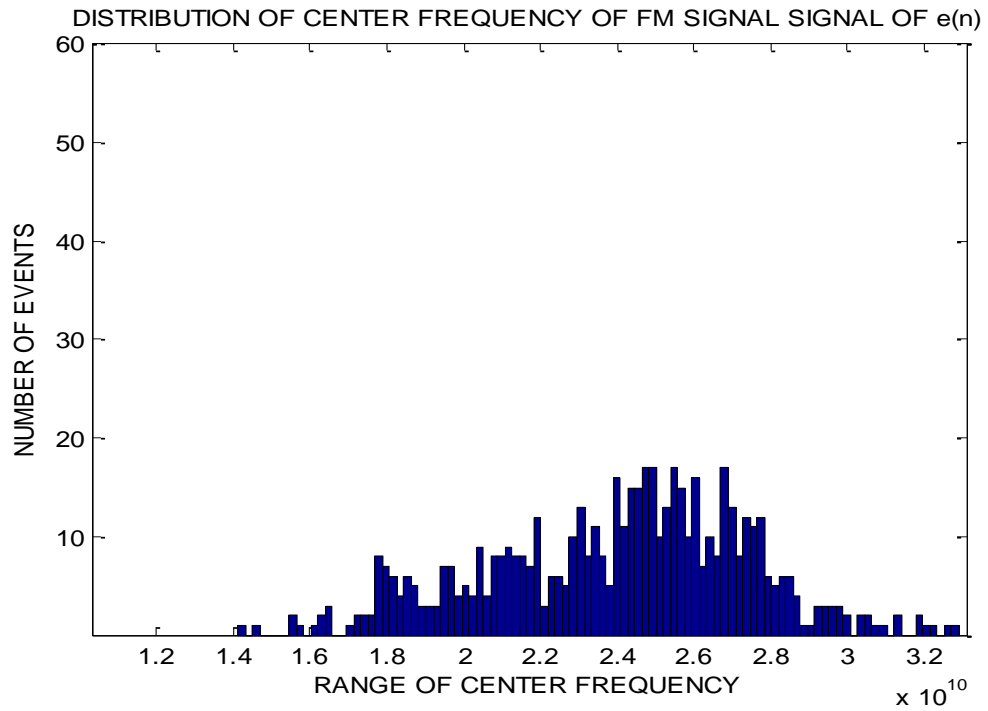


Figure 4.9: Distribution of center Frequency of the Lang-Kobayashi chaotic FM signal.

4.3 Ensemble mean Autocorrelation of Chaos Based Frequency Modulated Signals

In order to achieve high resolution of the target in range, the autocorrelation plot should be characterized by a sharp mainlobe at its center and successive side lobes must die out with increase in time lag. It is possible to roughly estimate the autocorrelation of the signal from a single realization of the chaotic signal as suggested elsewhere. However, it is preferable to lower the variance of the autocorrelation or spectrum by utilizing traditional approaches, such as the correlogram or periodogram. Our chosen methodology is to generate the local FM signal realizations, compute the biased time autocorrelation of each realization, and calculate the autocorrelation average bin by bin.

From time-frequency distribution of the respective FM signals, we consider the local FM signal that gives positive linear pattern of time-frequency distribution as N. By calculating the autocorrelation of each of N and averaging the response, the ensemble mean autocorrelation is obtained.

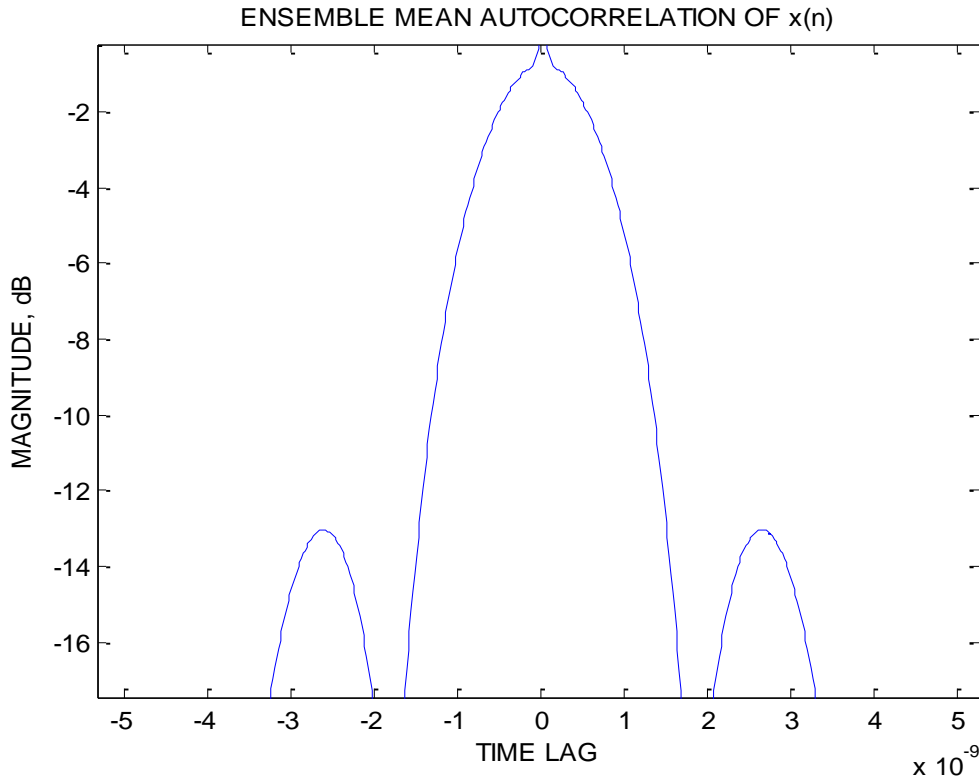


Figure 4.10: Ensemble mean autocorrelation of the Lorenz chaotic FM signal for reference parameter values.

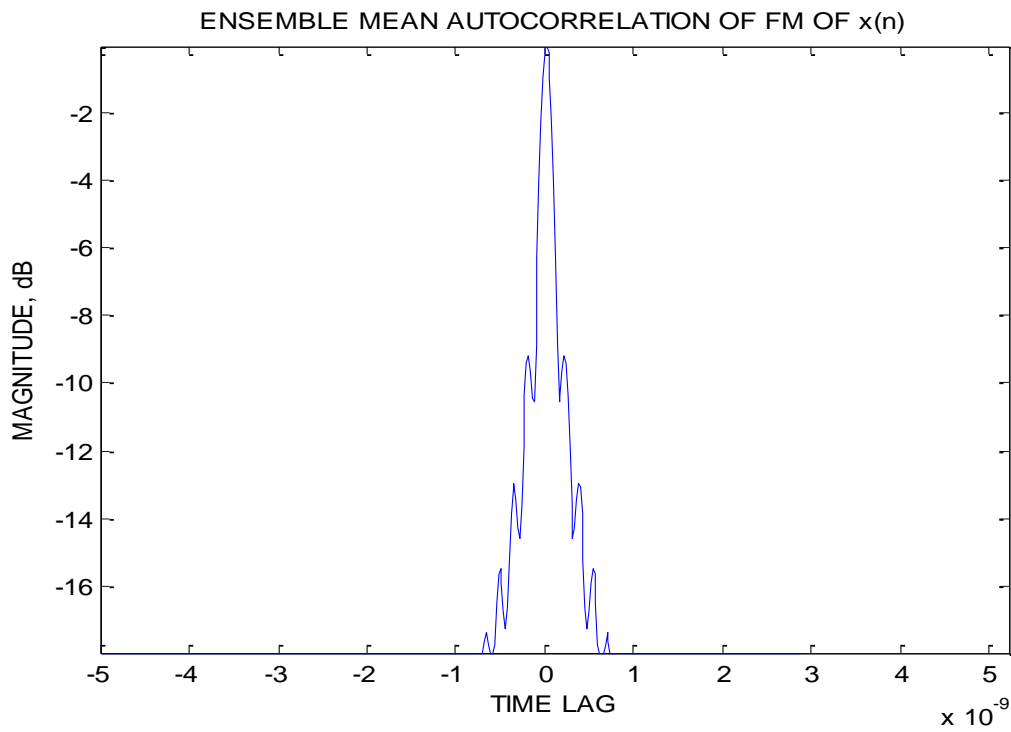


Figure 4.11: Ensemble mean autocorrelation of the Lorenz chaotic FM signal for optimized parameter values.

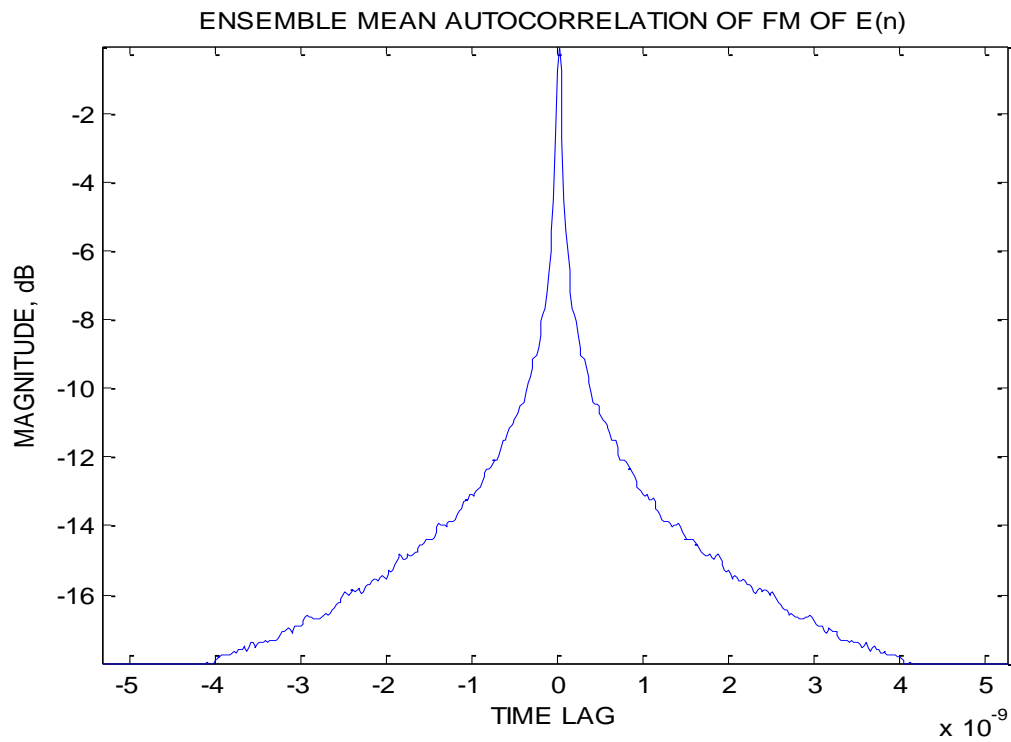


Figure 4.12: Ensemble mean autocorrelation of the Lang-Kobayashi chaotic FM signal.

Figure 4.10 and 4.11 shows the ensemble mean autocorrelation of the reference Lorenz chaotic FM signal and the optimized Lorenz chaotic FM signal of $x(n)$. Figure 4.12 shows the ensemble mean autocorrelation of the Lang-Kobayashi chaotic FM signal of $E(n)$. Figure 4.10 shows a very blunt mainlobe which is not desirable for the obtaining high resolution. From Figure 4.11, the autocorrelation of the optimized signal has very sharp mainlobe compared to the reference Lorenz chaotic FM signal which is desirable feature required in obtaining high resolution radar imaging applications [23]. Even the ensemble mean autocorrelation of the Lang-Kobayashi chaotic FM signal from Figure 4.12 has a blunt mainlobe compared to ensemble mean autocorrelation of the optimized Lorenz chaotic FM signal. The sidelobes of the autocorrelation should be shallow and die out with increase in time lag [24] as it is seen in all the three cases.

The density shows a peak at the mean and dies out as the variable moves away from the mean. The ensemble mean autocorrelation in all the three cases approximate quasi-Gaussian distribution as expected because the distribution of its corresponding chaotic signals also approximates the quasi-Gaussian distribution. Compared to all the three cases the optimized Lorenz chaotic FM signal has high decorrelation because of the high value of divergence in its phase component which shows effect on its correlation characteristics. Most importantly, the autocorrelation mainlobe width is inversely proportional to the bandwidth of the FM signal in all cases.

4.4 Ensemble mean Ambiguity Surface of Chaos Based Frequency Modulated Signals

Equation 3.18 conveniently summarizes the response of a matched filter to a point target that is delayed and Doppler-shifted with respect to expected target for which the matched filter is tuned. If radar is matched to a target at a particular range and velocity, ambiguity function or ambiguity surface gives information regarding the extent to which the radar can distinguish between that target and another target at respective range and velocities.

The ambiguity surface of each of the chaos based FM signal resembles a set of mountain ridges with positive slopes as shown in Figure 12. The bandwidth of the signal depends on the slope of the ambiguity surface. It is tested that if slope tends to unity, the bandwidth will be higher similar to chirp signal which has high bandwidth as chirp rate tends to unity.

We computed the average of the ambiguity surface using Equation 3.18 for the FM signals that gives corresponding positive linear pattern of time-frequency distribution. Figure 4.13 shows the ambiguity surface of the reference Lorenz chaotic FM signal of the Lorenz attractor and figure 4.14 shows the ambiguity surface of the optimized FM signal of the Lorenz attractor. The FM signals constructed in highly chaotic parameter space region have a wide range of signals to be transmitted with high bandwidth compared to the FM signal constructed in normal parameter space region. Figure 4.15 shows the ambiguity surface of the Lang-Kobayashi chaotic FM signal.

Each ambiguity surface has a prominent peak at the center of range as well as Doppler with minor sidelobes off the main axes. On average, the sidelobes on range-Doppler plane have a relative magnitude of $10\log_{10}(1/N)$ [17] with respect to peak. In the case of the reference Lorenz chaotic FM signal the range sidelobes occur at -12dB whereas Doppler sidelobes occur at -13dB. In the case of the optimized Lorenz chaotic FM signal the range sidelobes occur at -9 dB and Doppler sidelobes occur at -13.4dB. In case of the Lang-Kobayashi chaotic FM signal both the range and Doppler sidelobe occur at -13.4dB along the range axis at zero Doppler the feature sidelobes match the autocorrelation of the FM signal. Similar results can be obtained for negative slopes of time frequency plots, but the ambiguity surface has result with mountain ridges having negative slopes. The sidelobes adjacent to the main response peak can be lowered using windowing techniques.

Even though the autocorrelation of the optimized FM signal has more sidelobes than the autocorrelation of the reference Lorenz chaotic FM signal and the Lang-Kobayashi chaotic FM signal, because the main lobe width is sharp for the optimized FM signal, it gives high resolution in target

imaging. The corresponding range resolution for the optimized Lorenz chaotic FM signal and the Lang-Kobayashi chaotic FM signal is obtained as 0.99 cm, whereas the reference Lorenz chaotic FM signal resolution is obtained as 13.5 cm. Hence the optimized Lorenz chaotic FM signal and the Lang-Kobayashi chaotic FM signal gives better results compared to the reference Lorenz chaotic FM signal. Table 4.1. shows the different measures obtained for the reference Lorenz chaotic FM signal, the optimized Lorenz chaotic FM signal and the Lang-Kobayashi chaotic FM signals.

Table 4.1. Comparison of results obtained for different types of chaos based FM signal.

Measures	Reference Lorenz FM signal	Highly chaotic Lorenz FM signal	Lang-Kobayashi FM signal
Lyapunov exponents	1.01	26.15	0.61
Time-Bandwidth Product	50000.00	75000.00	55000.00
Mean Fractional bandwidth	0.80	1.05	1.10
Range sidelobe level	-13.00 dB	-9.00 dB	-13.4.00 dB
Bandwidth	1.10 GHz	15.15 GHz	15.00 GHz
Resolution	13.50 cm	0.99 cm	1.00 cm

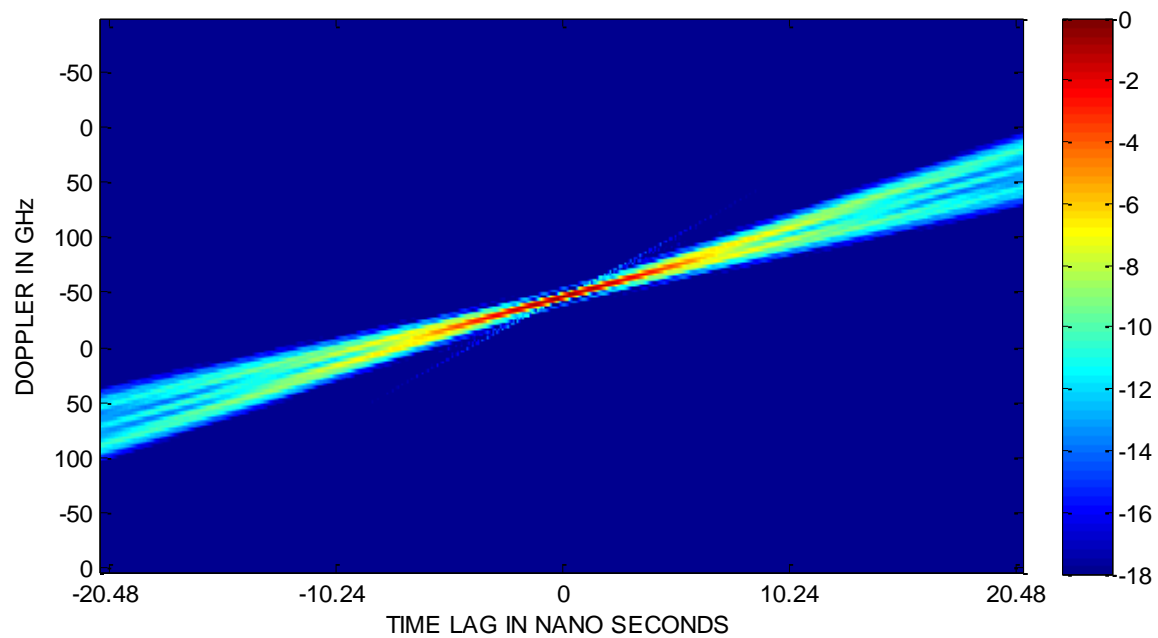


Figure 4.13: Ensemble mean ambiguity surface of the Lorenz chaotic FM signal for reference parameter values.

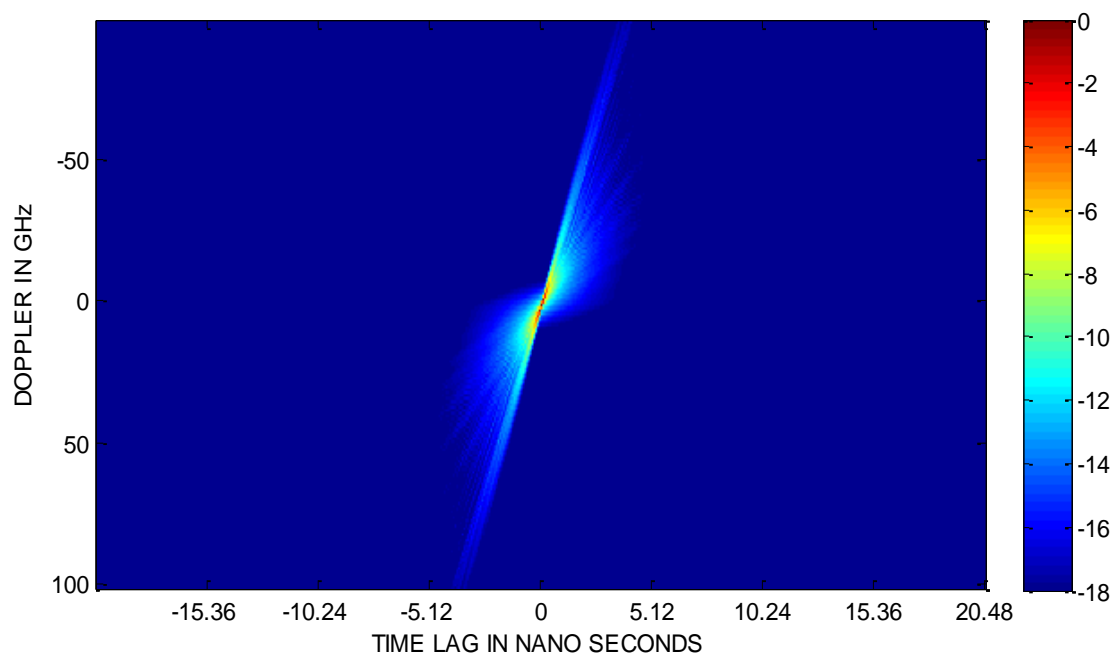


Figure 4.14: Ensemble mean ambiguity surface of the Lorenz chaotic FM signal for optimized parameter values.

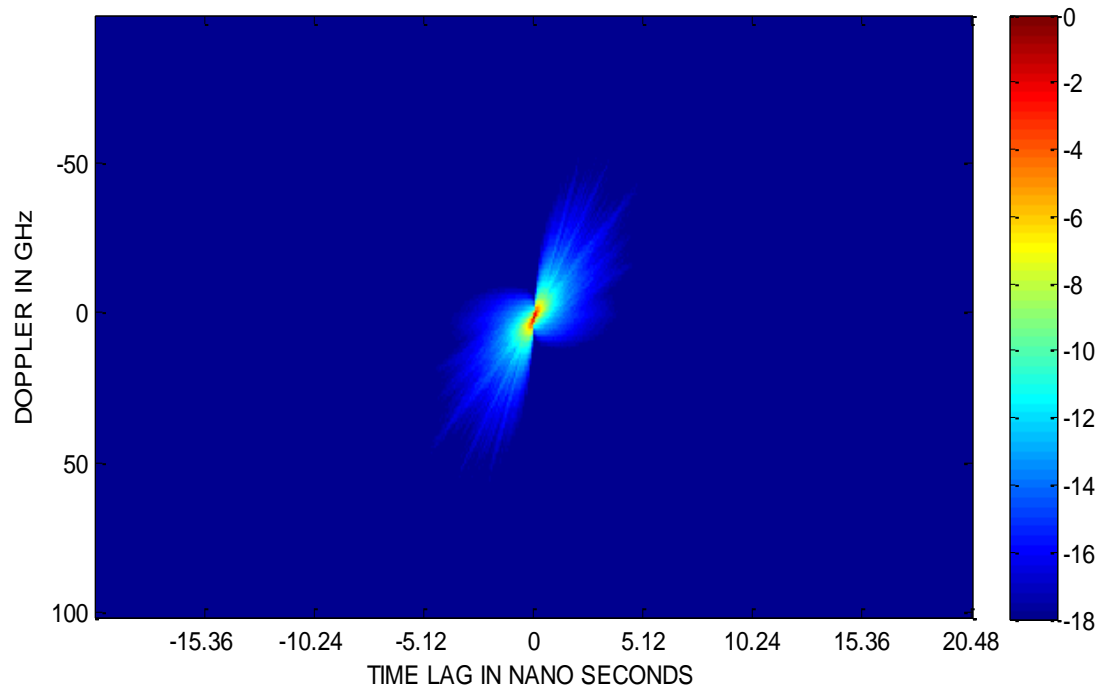


Figure 4.15: Ensemble mean ambiguity surface of the Lang-Kobayashi chaotic FM signal.

Chapter 5: Conclusions

Deterministic chaotic signals have been presented for the designing of wideband radar signals in high resolution applications. Chaotic signals which have random and bounded behavior were generated by using a set of non linear differential equations which are governed by a set of control parameters. For simplicity we chose the Lorenz system which has a set of three state variables x , y and z and three control parameters ρ , β , and σ . For comparison purpose we introduced another chaotic system called the Lang-Kobayashi attractor which has three state variables e , ϕ and z and two main control parameters L and η . Any one of the state variables x , y and z or e , ϕ and z are chosen as an instantaneous frequency to generate realizations of the wideband chaos based FM signal $s(n)$.

A technique for optimizing the bandwidth of the constructed FM signal is developed based on optimizing the Lorenz control parameter region. The method is based on exploiting highly chaotic parameter space region by varying control parameters as function of time. Considering parameter complexity we have introduced a compression factor such that the Lorenz attractor starts oscillating with high frequency. We observed that the FM signal constructed in the highly chaotic parameter space region behaves optimally compared to the FM signal constructed in normal parameter space region. The constructed Optimized Lorenz chaotic FM signal has similar characteristics as that of the Lang-Kobayashi chaotic FM signal.

The FM signals constructed from both the attractors are ergodic and wide sense stationary and the time samples exhibit an invariant probability distribution function. We noticed that the corresponding pseudo-phase space trajectories of the FM signal reveal themselves as a strange attractor that may take on the shape of a Mobius strip, disc or an extended disc, depending on the time evolution of the signal. The time frequency analysis of the FM signal shows that the spectrum is centered on a time-dependent carrier frequency. The carrier frequency continuously shifts in a linear pattern or

quadratic pattern exhibiting the fractal nature same as that of a chaotic signal. We observed that the pseudo-phase space trajectory of the local FM signal achieves the shape of a Mobius strip whenever it is a linear pattern and it attains the shape of an extended disc whenever it is quadratic pattern. Depending upon slope and length of linear pattern the pseudo phase attractor of FM signal evolves as a Mobius strip with more number of orbits. The corresponding spectra have an ultra wide bandwidth in nature.

Based on the shifts in carrier frequency as observed in time-frequency distribution, frequency agility has been achieved with a finite number of discrete wide bandwidths of range varying more than 150 MHz with in ultra- high wide bandwidth. We estimated the time average autocorrelation of both the chaos based FM signals. In particular we determined that the autocorrelation of the optimized Lorenz chaotic FM signal has a very sharp mainlobe with sidelobes dying out quickly with increase in time lag. The autocorrelation of the Lang-Kobayashi attractor has no sidelobes and its samples are high decorrelated. The time average autocorrelation in both cases approximate quasi-Gaussian shape as expected because the distribution of its corresponding chaotic signal has quasi-Gaussian distribution.

The fractional bandwidth of the chaos based FM signal, in particular the optimized Lorenz chaotic FM signal has a value above 1.0 which shows the wideband characteristics of constructed FM signal nature. The Time-bandwidth product of the chaos based FM signal, also in particular for the optimized Lorenz chaotic FM signal is way above 75,000 which is highly desirable for signal compression techniques. Using ensemble mean, the ambiguity surfaces for both the types of chaos based FM signals has been computed. The ambiguity surface shows that the optimized FM signal has more range of mountain ridges compared to the reference Lorenz chaotic FM signal with positive slopes depending on slopes of time-frequency distribution. Also the ambiguity surface of the Lang-Kobayashi has wide range of mountain ridges which is desirable property. We also proved that the bandwidth of the FM is high whenever there is more slope in the ambiguity surface. Thus the range resolution obtained for the FM signal in the normal parameter space region is 13.5 cm while in highly chaotic parameter

space region and for the Lang-Kobayashi chaotic FM signal is 0.99 cm. Hence the FM signal constructed in the highly chaotic parameter space region has higher bandwidth and high resolution.

Future work includes the analysis of chaos based FM signal in presence of noise. Implementation of the Lorenz chaotic chaotic FM signal in real time application has already been started. We plan to extend the work by simulating wider region of parameter space region and to estimate the cutoff value of the Lyapunov exponent after where the constructed FM signal behaves similarly.

References

1. Julian. C. Sprott, [Chaos and time series analysis], Oxford University Press, Edition. 1 (2003).
2. M. P. Kennedy, R. Rovatti and G. Setti, "Chaotic Electronics in Telecommunication," CRC Press, 2000.
3. J. C. Toomay, "Radar Principles for the Non-Specialists," Von N. Reinhold, Edition. 2, 1989.
4. J. Minkoff, "Signals, Noise and active sensors," A Wiley-Interscience Publication, Edition. 1, New York (2001).
5. J. S. Son, G. Thomas, B. C. Flores, "Range-Doppler Radar Imaging," Artech House, Edition. 1, Boston, 2001.
6. D. R. Wehner, "High Resolution Radar," Artech House, Edition. 1, Boston, 1987.
7. B. M. Horton, "Noise-modulated distance measuring systems," Proceedings of IRE, vol. 49, pp. 821-828, May 1959.
8. L. Guosui, G. Hong, and S. Weimin, "Development of random signal radar," IEEE transactions on Aerospace and Electronic System, Vol. 35, No. 3, pp. 770-777, July 1999.
9. R. M. Narayanan and D. C. Bell, "Theoretical aspects of radar imaging using stochastic waveforms," IEEE transactions on Signal Processing, Vol. 49, No. 2, pp. 394-440, July February 2001.
10. B. C. Flores., E. A. Solis., G. Thomas., "Assessment of chaos-based FM signals for range-Doppler imaging," Radar, Sonar and Navigation, IEE Proceedings, 150(4), 313-322 (2003).
11. B. C. Flores., E. A. Solis., G. Thomas., "Chaotic signals for wideband radar imaging," Proc. SPIE 4727, 100-111 (2002).
12. A. Ashtari, G. Thomas, B. C. Flores, H. Garces, "Radar Signal Design Using Chaotic Signals," "IEEE transactions on Waveform Diversity and Design Conference, 353-357 (2007).
13. A. Ashtari., G. Thomas., B. C. Flores., and W. Kinsner., "Sufficient condition for Chaotic Maps to show Chaotic Behavior after frequency modulation," IEEE transactions on Aerospace and Electronic Systems 44(3), 1240-1248 (2007).
14. G. Lind. "A Simple Approximate Formula for Glint Improvement with Frequency Agility," IEEE trans. on Aerospace and Electron.Sys., Vol. 8 (1972), pp. 854-855.

15. Chandra S. Pappu and Benjamin C. Flores, "Generation of high-range resolution radar signals using the Lorenz chaotic flow," Radar Sensor technology XIV, Proc. SPIE 7669, (2010).
16. Berenice Verdin "Characterization of High Resolution Range and Doppler chaotic Ladar", University of Texas at El Paso.
17. Benjamin C. Flores and Berenice Verdin, "Characterization of high resolution range and Doppler LADAR," Lidar Remote Sensing for environment Monitoring technology X, Proc. SPIE 7460, (2009).
18. C. Sparrow, "The Lorenz Equations: Bifurcations, Chaos and Strange Attractors," Springer-Verlag, New York, 1982.
19. Skolnik, M. I., [Introduction to radar systems], McGraw-Hill, Edition.3, New York (2001).
20. Alberto Leon-Garcia, "Probability and Random processing for Electrical Engineering," Addison Wesley, Edition. 1, 1989.
21. Henry Starks, John W. Woods, "Probability and Random Processes with application to signal processing," Pearson education, Edition. 3, 2006.
22. A. Papoulis., "Probability, Random Variable, and Stochastic Processes," McGraw-Hill, Edition.3, New York, 1984.
23. Alan V. Oppenheim., Ronald W. Schaffer, "Digital Signal Processing," Prentice-Hall, Edition. 2, 1999.
24. Slamani, M., Weiner, D., Tsao, T., Varshney, P., Schwarzlander, H., and Borek, S.: 'Continuous-time continuous-frequency and discrete-Time discrete-frequency ambiguity functions'. Proc. IEEE-SP Int.Symp. on Time-frequency and time-scale analysis, Victoria, BC, Canada, 1992, pp. 501-504.
25. Bruce A. Carlson, "Communication Systems," McGraw-Hill Book Company, Edition. 3, 1986.

Vita

Chandra Sekhar Pappu was born on April 26, 1987 in Amalapuram, AP. He is the first son of Mr. and Mrs. P. S. R. Murthy. He graduated with a B. Tech. degree in Electrical and Electronics Engineering in 2008 from the Guru Nanak Engineering College which is affiliated with Jawaharlal Nehru Technological University. As an undergraduate he gave multiple presentations in the area of digital signal processing and communications. He presented two papers at the International conference for Systemics, Cybernetics and Informatics where one of his presentations was awarded as best presentation. Mr. Chandra S. Pappu joined the University of Texas El Paso (UTEP) in 2008. He worked as a graduate industry intern for Lockheed Martin Company. He is currently working under the direction of Dr. Benjamin C. Flores, researching chaotic signals for wideband radar systems. He presented his research results at the SPIE conference in Radar Sensor Technology.

Permanent address: 1-4-295, New Maruthi Nagar East
Hyderabad, AP, 500036

This thesis was typed by the Chandra Sekhar Pappu.